AD-A019 098

TEST PROCEDURES FOR EVALUATING TERMINAL PROTECTION DEVICES USED IN EMP APPLICATIONS

Robert L. Williams, Jr.

Harry Diamond Laboratories

Prepared for:

Defense Nuclear Agency

June 1975

Best Available Copy

UNCLASSIFIED

SECURITY CLASSIFICATION OF THIS PAGE (When Data Entered)

REPORT DOCUMENTATION PAGE		READ INSTRUCTIONS BEFORE COMPLETING FORM
1. REPORT NUMBER HDL-TR-1709	2. GOVT ACCESSION NO.	3. RECIPIENT'S CATALOG NUMBER
4. TITLE (and Subtitle) Test Procedures for Evaluating Terminal Protection Devices Used in EMP Applications		5. TYPE OF REPORT & PERIOD COVERED Technical Report
		6. PERFORMING ORG. REPORT NUMBER
7. AUTHOR(s) Robert L. Williams, Jr.		8. CONTRACT OR GRANT NUMBER(s)
9. PERFORMING ORGANIZATION NAME AND ADDRESS Harry Diamond Laboratories 2800 Powder Mill Road Adelphi, MD 20783		10. PROGRAM ELEMENT, PROJECT, TASK AREA & WORK UNIT NUMBERS Prog. Ele. 6.27.04.H
11. CONTROLLING OFFICE NAME AND ADDRESS Director Defense Nuclear Agency Washington, DC 20305		12. REPORT DATE June 1975
		13. NUMBER OF PAGES 54
14. MONITORING AGENCY NAME & ADDRESS(if different from Controlling Office)		15. SECURITY CLASS. (of this report) Unclassified
		15a. DECLASSIFICATION/DOWNGRADING SCHEDULE

16. DISTRIBUTION STATEMENT (of this Report)

Approved for public release; distribution unlimited.

17. DISTRIBUTION STATEMENT (of the abstract entered in Block 20, if different from Report)

18. SUPPLEMENTARY NOTES HDL Proj. No. E044E2 AMCMS Code-691000.22.10922
This work was completed in July 1974.
This research was sponsored by the Defense Nuclear Agency under Subtask R99QAXEB099, Work Unit 41, Circuit Protection and Hardened Networks.

19. KEY WORDS (Continue on reverse side if necessary and identify by block number)

EMP
Terminal protectors
Electromagnetic suppression devices

20. ABSTRACT (Continue on reverse side if necessary and identify by block number)

Certain commercially available components have been tested to establish test procedures for characterizing terminal protection devices used in electromagnetic-pulse (EMP) applications. The devices tested include spark gaps, filters, avalanche diodes, and various other nonlinear components. Square pulses of 50- and 500-nsec duration and up to 11 kV in amplitude, with rise times of 2 to 4 nsec, were applied to the devices. Response time and energy leakage were recorded for each test. Insertion loss and approxi-

DD FORM 1473 1 JAN 73 EDITION OF 1 NOV 65 IS OBSOLETE

UNCLASSIFIED

SECURITY CLASSIFICATION OF THIS PAGE (When Data Entered)

1

mate failure level were measured for each device. Results are presented in tabular form. The devices that appear suitable for terminal protection include spark gaps, some filters, and some semiconductor devices with breakdown voltage less than 50.

PREFACE

This work was sponsored by the Defense Nuclear Agency under subtask R99QAXEB099, Theoretical and Experimental EMP Hardening. Several HDL staff members have contributed toward this program. Initial planning of the test sequences was carried out by Herbert S. McBride (formerly of HDL). The devices were acquired and tested by William C. Gray. George Gornak directed the overall program.

TABLE OF CONTENTS

APPENDICES

ILLUSTRATIONS

TABLES

1. INTRODUCTION

1.1 Statement of Problem

Electromagnetic pulses (EMP) generated by the detonation of nuclear weapons can induce large voltages and currents in wires, cables, and antennas connected to sensitive electrical and electronic equipment thereby causing momentary or permanent disruption in the operation of this equipment. While grounding and shielding techniques can effectively divert the direct EMP wave, the induced energy must be prevented from entering via the terminals of the equipment. Thus, there is a need for terminal protection devices (TPD's), both for retrofitting existing equipment and for use in the design of new equipment.

The TPD associated with a given terminal is to be connected between the terminal and ground, thus providing an alternate path for the incident transient current and reflecting some, or perhaps most, of the energy away from the protected equipment. The more important characteristics of TPD's follow:

(a) The insertion loss incurred by connecting the TPD should not be so large as to interfere with the normal operation of the system. For practical purposes, this may limit the insertion loss to ~1 dB over the frequency range of interest. In some systems, the TPD capacitance could be limited to a few picofarads.

(b) The TPD should be capable of absorbing a large amount of energy without being damaged thereby. A protection philosophy that allows the protective element to be damaged in the process of providing protection is inadvisable. There may be no opportunity for replacement during an attack.

(c) The TPD should be inoperative for input voltages below the desired protection level and should respond rapidly to inputs that exceed this level, passing from low-to-high conductivity. The speed with which this transition takes place may be called the response time of the TPD. During this transition the TPD voltage may exceed the protection level by a substantial amount--called overshoot--which should be minimal in amount and time. The requirements of the system being protected will largely establish limits for the overshoot.

(d) After the initial overshoot, the TPD should limit the transient voltage to a reasonably small range near the protection level, more or less independent of the current passing through the device. What constitutes a reasonable voltage range will be determined largely by the requirements of the system being protected.

Preceding page blank

Quantitatively, the desired characteristics of terminal protection devices can be derived from the parameters of voltages and currents induced in the antennas, wires, and cables of the system, and from the properties of the system to be protected. Based on field and laboratory testing experience, some standards for TPD's have been tentatively established. First, the TPD should be able to suppress a voltage transient of about 10 kV, which implies a maximum short-circuit current of about 400 A in a 50-Ω system. Second, the TPD should switch from the low- to the high-conduction state in less than 5 nsec. Third, the TPD should be able to maintain this high-conduction state for at least 500 nsec.

1.2 Objectives

Primarily, the first-phase objectives of the test program were to:

(a) Develop experimental techniques for characterizing and evaluating TPD's that have potential usefulness in EMP applications;

(b) Collect experimental data (data bank) on the insertion losses, energy absorbing capacities, response times, and voltage limiting effectiveness of the candidate TPD's, so that their usefulness in EMP applications can be determined; and

(c) Develop insertion methods that optimize the effectiveness of TPD's in specific system applications. These results were expected to generate other benefits. For example, it was anticipated that selection criteria, specifications, and acceptance tests for TPD's could be derived from this data base.

1.3 Selection of Devices

Many characteristics of electrical components ultimately determine their suitability for terminal protection devices, such as switching time, power-handling capability, weight, cost, size, temperature limits, frequency limits, ruggedness, and hermetic sealing. Some of these characteristics are not known or at least have not been published by the manufacturers. In many cases, the pulse-power-handling capability has not been published because it is not an important consideration in the normal usage of the device. The devices tested in this program were selected on the basis of a technical-literature survey and from suggestions of those experienced in the field.

2. TEST PROCEDURE

To evaluate the effects of pulse testing, it is necessary to compare certain electrical properties of each device before the pulse test with the same properties measured after the pulse test. It was decided that measurements of insertion loss and current-voltage characteristics would be adequate for this work. Therefore, before high voltage pulse testing, each device was examined on a spectrum analyzer to measure its insertion loss from 0.01 to 100 MHz, and each device (except spark gaps and filters) was also examined on a curve tracer.

After being pulsed each device was again tested on the curve tracer and/or spectrum analyzer. Comparisons of pre-test and post-test data were then used to assess component degradation. This procedure was followed for each pulse amplitude.

In the initial round of tests the pulse width was 50 nsec and the amplitudes--measured across a matched 50-Ω load with no TPD in place--were 1, 3.8, 8.2, and 11 kV. When post-pulse tests indicated that a device had been damaged, no further pulses were applied to that device. A listing of the undamaged or surviving devices was completed after the tests.

In the second series of tests (which was applied to the survivors of the first tests), the pulse width was increased to 500 nsec, and the amplitudes were 3.5, 7.5, and 11 kV. These additional tests were, of course, intended solely to study the energy dissipation capacities of the devices to a somewhat greater extent. The 3.5-kV, 500-nsec pulse was chosen to be roughly equivalent to the 11-kV, 50-nsec pulse as far as semiconductor-device-junction heating is concerned, assuming that both pulse widths lie in the range of applicability of the Wunch[1] model for semiconductor junction damage due to thermal effects.

The highest test level of 11 kV was chosen because it was the maximum available and because it appeared to be a good practical test.

The logic flow diagram for these studies is shown in figure 1.

3. INSTRUMENTATION

3.1 Pulsers

The pulse generators used in these experiments were of the charged coaxial transmission-line type, having two in-line spark gaps to create fast rise times. The gaps were operated in a nitrogen atmosphere, and the pressure and gap spacing were varied to give the fastest practical rate of rise for each pulse amplitude.

[1] Wunch, D. C., and Bell, R. P., IEEE Trans. on Nucl. Sci., Vol. NS-15, No. 6, Dec 1968.

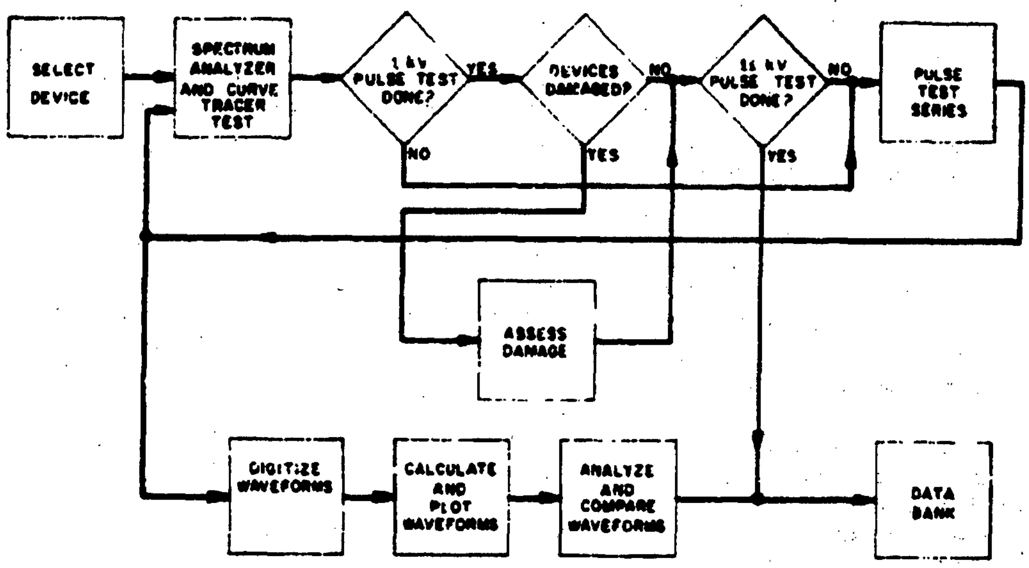

Figure 1. Logic flow chart for pulse testing and evaluation of terminal protection devices (TPD).

One line produced 50-nsec pulses with amplitudes of 1 to 11 kV into a matched 50-Ω load. Generally, the rise times obtainable with this pulser were 2 to 4 nsec, measured from 10 to 90 percent of maximum; but at the highest voltage, there was a 1- to 2-nsec decrease in rise time. This line was [illegible] and required a resistive matching section to connect to the measurement sections. The match was poor at the lowest voltage but reasonably good at the higher voltages.

The other transmission line produced 500-nsec pulses with amplitudes of 1 to 11 kV into a matched 50-Ω load. The rise times obtained with this pulser were about 2 to 4 nsec, measured from 10 to 90 percent of maximum. Shorter rise times could perhaps have been achieved, but no effort was made to do so because the object of using 500-nsec pulses was to investigate damage levels more extensively. This line was a standard 3-1/8-in. o.d. rigid copper transmission line and 50 Ω throughout. Two taper sections reduced the 3-1/8-in. diameter to 7/8 in. to fit the measurement section.

A schematic diagram of these pulse generators is shown in figure 2. The theory of pulse-forming lines is reviewed in appendix A, which follows the treatment of Goldman.

Goldman, Stanford, "Laplace Transform Theory and Electrical Transients," Dover, NJ, 1949.

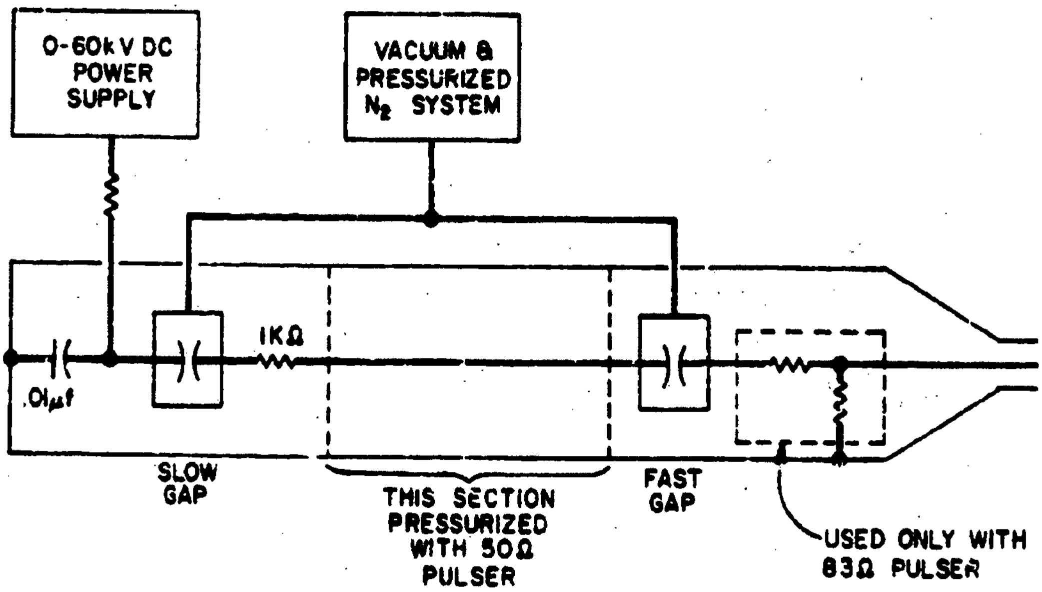

Figure 2. Schematic diagram of pulse generators used for testing of terminal protection devices.

2.2 Measurement Section

The voltage across and the current through the load were determined by means of special instrumentation sections placed before and after the load, as shown schematically in figure 3. The voltage was measured with a resistive probe and attenuator, which provided a matching network between the 50-Ω instrumentation section and the 125-Ω input of a Tektronix 519 oscilloscope. A series of plug-in networks was used to provide further attenuation when necessary. This voltage measurement was made on the downstream side of the device under test so that only the transmitted wave was obtained.

The current was determined by observing the voltage drop across a small resistance internal to the instrumentation section and concentric with the conductors of the 50-Ω line. Several resistance values were available in the 0.04- to 0.4-Ω range, so that the voltage drop could be adjusted to a convenient range. The current was measured ahead of the device under test; thus, the measured values include the current through the 50-Ω terminator. This terminator current is relatively small, except when the device does not conduct; it was then generally ignored.

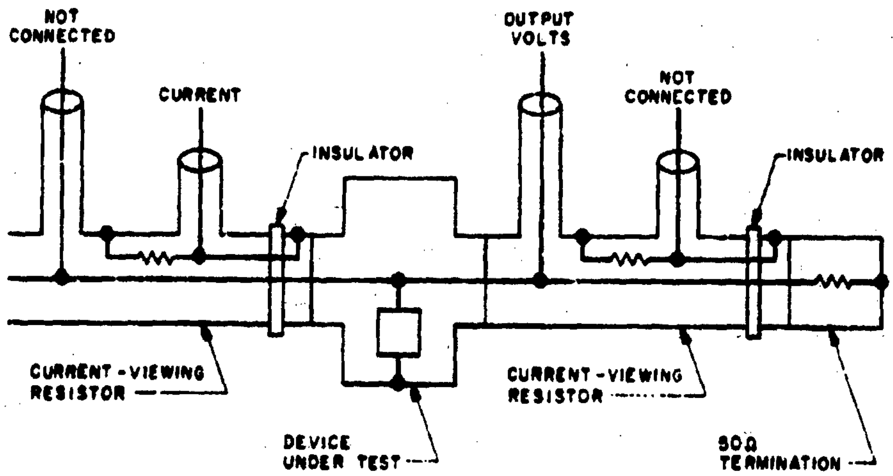

Figure 3. Schematic diagram of measurement sections used in pulse testing the terminal protection devices.

3.3 Oscilloscopes and Cameras

Voltage and current pulses were recorded by two Tektronix 519 oscilloscopes equipped with Tektronix C-27 cameras with 1:1 lenses, using Polaroid type 410 film, ASA 10,000. The inputs to these oscilloscopes were applied directly to the deflection plates, which permitted rise times of 0.28 to 0.30 nsec. The combination of P11 phosphor in the CRT and ASA 10,000 film allowed clear recording of all pulses, even when the oscilloscope sweep speed was 5 nsec/cm. Photographs with a sweep speed of 2 nsec/cm were possible but added no useful information.

3.4 Curve Tracer

Current-voltage characteristics were generally obtained, using a Tektronix 576 curve tracer equipped with a Tektronix C-12 camera and Polaroid type 107 film, ASA 3000. In some cases a Tektronix 7904 oscilloscope equipped with a Tektronix 7CT1N curve tracer plug-in and a Tektronix C-31 camera were substituted for the above combination. In such cases it was necessary to photograph the forward and reverse curves separately, which presented no difficulty.

Since these curves are swept out at such a low frequency (they are commonly called d-c characteristics), the devices were simply attached to the curve tracer in a convenient fashion.

3.5 Spectrum Analyzer

Insertion-loss measurements were made with a Hewlett-Packard spectrum analyzer system, which included a model 8443A tracking generator-counter, a model 8552A spectrum analyzer IF section, a model 8553A spectrum analyzer rf section, and a model 141S display section. The camera employed was developed by Fairchild for the Defense Atomic Support Agency (now the Defense Nuclear Agency).

Two photographs made for each device covered approximate frequency ranges of 0 to 10 MHz and 0 to 100 MHz. The vertical resolution of this instrument is 10 dB/div, so that variations of less than ~ 1 dB were difficult to measure.

The device under test was mounted in the same housing for these measurements as for the pulse tests. The 0-dB reference was established by making the same observations on an empty housing. The test apparatus is shown schematically in figure 4.

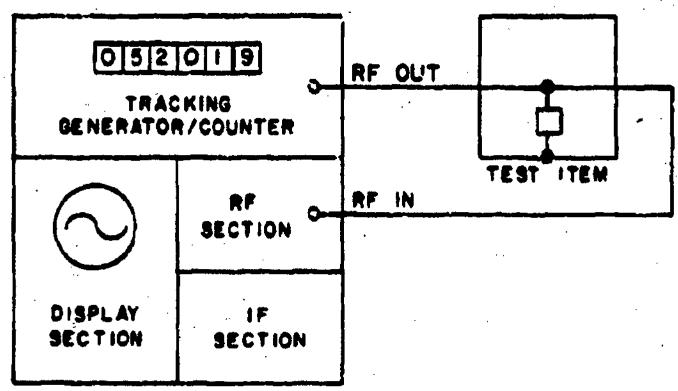

Figure 4. Schematic diagram of spectrum analyzer test.

4. RESULTS

4.1 Important Observables

4.1.1 Insertion Loss

The frequency response of a device under normal operating conditions, or its insertion loss, was measured as indicated in section 3.5. This gives the direct amount of loading of a 50-. circuit by the device in its nonconducting state. It was found that the insertion loss can be well represented by values at a few frequencies. We chose 5, 10, 50 and 100 MHz, largely as a matter of convenience, but the choice is not critical. These results are presented in table I, along with 3-dB points (where these could be determined) for all devices tested. The frequencies at which the loss passed through 1 dB would perhaps have been more useful, but the resolution of the spectrum analyzer was of such that these points could not be determined with a reasonable accuracy. The insertion losses and 3-dB frequencies listed in table I* are averages over the sample of that particular device type. The sizes of these samples are listed in table II.*

As table I indicates, many semiconductor devices would be useful only at low frequencies because of their high-insertion loss. The more obvious examples are silicon-controlled rectifiers (SCR's) and some avalanche diodes. The case of the avalanche diode is particularly illuminating because the same properties that cause a diode to show high-insertion loss--that is, large junction area and small depletion width--also allow it to survive larger input transients. The depletion width, of course, derives from the impurity concentration, and a higher level of impurity carriers means that more current can be impressed without excessive heating of the crystal.

At the other extreme, spark gaps generally exhibit little or no measurable insertion loss.

4.1.2 Survivability

The approximate level at which a device was damaged was determined by comparing pre- and post-pulse curve tracer and spectrum analyzer photographs. Damage was defined in this context as any significant difference between the two sets of photographs. This damage was generally evidenced by an increase in leakage current, for example. In extreme cases, the device either opened or shorted. It turned out that the insertion-loss curves were not often useful for damage evaluation, although they did sometimes confirm conclusions based on curve-tracer photographs. When the device was destroyed, as indicated by the curve tracer, it was occasionally noted that the insertion loss had markedly increased; and in rare cases where curve-tracer photographs were not available this fact was of some value.

*These tables are included with tabulated data on pp. 18 through 36.

INDEX TO TABLES

	Table I	Table II	Tables III & IV
Preset crowbar, dc	x	x	x
Hybrid SCR crowbar	x	x	x
Avalanche diode	x	x	x
Bipolar diode	x		
Microwave switching diode	x		
PIN DIODE			
Pulse shaping diode	x		
Silicon-controlled rectifier	x		
Diode ac switch	x	x	x
Biased Zener-like suppressor			
Thyristor	x		
SPARK GAPS			
Gas-tube arrester	x	x	
Spark gap	x	x	
Miniature gap	x	x	
Preionized gap	x	x	
FILTERS			
Bandpass filter	x	x	
Crystal bandpass filter	x	x	
EMI filter	x	x	
RFI/EMI filter	x	x	
Lossy-line filter	x	x	

MANUFACTURERS OF DEVICES REPORTED IN TABLES.

ALPHA	Alpha Industries, Inc Woburn, MA
DALE	Dale Electronics, Inc East Highway 50 Yankton, SD 57078
ECC	ECC Corporation Box 669 Euless, TX 76039
EG&G	EG&G, Inc Electronic Products Group 35 Congress Street Salem, MA 01970
GE	General Electric Semiconductor Products Department Electronics Pk. Syracuse, NY 13201
GHZ	GHZ Devices, Inc Kennedy Drive North Chelmsford, MA 01863
GSI	General Semiconductor Industries, Inc P.O. Box 3077 Tempe, AZ 85281
INT. RECT.	International Rectifier Semiconductor Division 233 Kansas Street El Segundo, CA 90245
JOSLYN	Joslyn Electronic Systems P.O. Box 817 Goleta, CA 93017
LUNDY	Lundy Electronic & Systems, Inc Glen Head, NY 11545
MCG	MCG Electronics 279 Skidmore Road Deer Park, NY 11729

MANUFACTURERS OF DEVICES REPORTED IN TABLES. (CONT'D)

M. ASSOC.	Microwave Associates, Inc Northwest Industrial Park Burlington, MA 01803
MOTOROLA	Motorola Semiconductor Products 5005 E. McDowell Road Phoenix, AZ 85008
RCA	Radio Corporation of America RCA Solid State Division Rt. 202 Somerville, NJ 08876
RTRON	Rtron Corporation P.O. Box 743 Skokie, IL 60076
SIEMENS	Siemens Corporation 186 Wood Avenue South Iselin, NJ 08830
SPEC. CONT.	Spectrum Control, Inc 152 East Main Street Fairview, PA 16415
TEXSCAN	Texscan Microwave Products 7707 Records Street Indianapolis, IN 46226
TII	Telecommunications Industries, Inc 1375 Akron Street Copiague, L.I., NY 11726
TMC	TMC Systems (Ariz), Inc 930 West 23rd Street Tempe, AZ 85281
TRANSTECTOR	Transtector Systems 532 Monterey Pass Road, P.O. Box 676 Monterey Park, CA 91754
UNITRODE	Unitrode Corporation 580 Pleasant Street Watertown, MA 02712
USCC	U.S. Capacitor Corporation 2151 N. Lincoln Street Burbank, CA 914504

TABLE I. INSERTION LOSS INDUCED IN A 50-Ω SYSTEM BY EACH COMMERCIAL DEVICE TESTED. (LOSSES ARE TABULATED AT 5, 10, 50, AND 100 MHz. ALSO INCLUDED ARE 3-dB POINTS, WHERE THE LOSSES COULD BE DETERMINED.)

Mfr*	Type	Description	V_B (V)	Insertion loss in decibels at (MHz) 5	10	50	100	3 dB Points (MHz) Low	High
MCG	LVC-1PA-6.8	Preset Crowbar, dc	6.8	18	28	18	14	-	0.7
"	LVC-1PA-10	"	10	14	22	18	14	-	1.3
"	LVC-1PA-15	"	15	16	26	17	13	-	1.1
"	LVC-1PA-20	"	20	14	22	18	13	-	1.2
"	LVC-1PA-50	"	50	6	12	20	14	-	3.4
"	LVC-1PA-100	"	100	2	6	30	15	-	7
"	LVC-1PA-150	"	150	1	6	30	15	-	7.4
"	LVC-1PA-200	"	200	1	4	27	16	-	8
TRANS-TECTOR	VH11DC1	Hybrid SCR crowbar	11	0	1	2	3	-	100
"	VH16.5DC1	"	16.5	0	0	1	3	-	100
"	VH30DC1	"	30	0	0	1	3	-	100
"	VH50DC1	"	50	0	0	0	1	-	-
"	VH5DC1	"	5	0	0	0	3	-	100

*See table IV for manufacturers names.

TABLE I. INSERTION LOSS INDUCED IN A 50-Ω SYSTEM BY EACH COMMERCIAL DEVICE TESTED. (LOSSES ARE TABULATED AT 5, 10, 50, AND 100 MHz. ALSO INCLUDED ARE 3-dB POINTS, WHERE THE LOSSES COULD BE DETERMINED.) (Cont'd)

Mfr*	Type	Description	V_B (V)	Insertion loss in decibels at (MHz) 5	10	50	100	3 dB Points (MHz) Low	High
DALE	LVP-6/6.2V	Avalanche diode	6.2	27	21	9	6	-	-
"	LVP-6/7.5V	"	7.5	26	20	9	6	-	-
"	LVP-6/9.1V	"	9.1	26	20	8	6	-	-
"	LVP-6/11V	"	11	27	24	8	6	-	-
"	LVP-6/13V	"	13	28	23	9	6	-	-
GSI	1N5017	"	7.5	10	18	10	6	-	1.5
"	1N5020	"	10	9	16	12	8	-	1.5
"	1N5042	"	50	1	4	24	11	-	8
"	1N5051	"	100	0	1	18	13	-	10
"	1N5344B	"	8.2	12	19	16	10	-	1
"	1N5369B	"	51	1	4	27	10	-	8
"	1N5378B	"	100	0	2	16	12	-	16
"	1N5388B	"	200	0	2	19	11	-	16

*See table IV for manufacturers names.

TABLE I. INSERTION LOSS INDUCED IN A 50-Ω SYSTEM BY EACH COMMERCIAL DEVICE TESTED. (LOSSES ARE TABULATED AT 5, 10, 50, AND 100 MHz. ALSO INCLUDED ARE 3-dB POINTS, WHERE THE LOSSES COULD BE DETERMINED.)(Cont'd)

Mfr*	Type	Description	V_B (V)	Insertion loss in decibels at (MHz) 5	10	50	100	3 dB Points (MHz) Low	High
MOTOROLA	IN1518	Avalanche diode	3.9	10	18	16	9	-	1.4
"	IN5262	"	52	1	2	4	16	-	40
"	IN5281	"	200	0	0	0	2	-	-
"	IN5271	"	100	0	0	0	6	-	80
"	IN5221	"	2.4	2	6	20	12	-	6.6
"	IN5240	"	10	0	1	13	16	-	16
"	IN1523	"	10	1	5	23	12	-	8.5
"	IN745	"	200	0	0	0	2	-	-
"	IN1799	"	150	0	0	5	24	-	30
"	IN1802	"	200	0	0	4	16	-	30
"	IN1788	"	51	0	2	14	18	-	1.4
RCA	40655	Silicon-controlled rectifier	500	1	2	4	9	-	30
"	40654	"	250	2	2	5	10	-	15
ECC	GT-40	Diode ac switch	43	0	0	0	5	-	90

*See table IV for manufacturers names.

TABLE I. INSERTION LOSS INDUCED IN A 50-Ω SYSTEM BY EACH COMMERCIAL DEVICE TESTED. (LOSSES ARE TABULATED AT 5, 10, 50, AND 100 MHz. ALSO INCLUDED ARE 3-dB POINTS, WHERE THE LOSSES COULD BE DETERMINED.) (Cont'd)

Mfr*	Type	Description	V_B (V)	Insertion loss in decibels at (MHz)				3 dB Points (MHz)	
				5	10	50	100	Low	High
GE	ST-2	"	32	0	0	0	2	-	-
RCA	1N5411	"	29	0	1	28	8	-	14
MCG	LVC-1Z-1/4.9A	Biased Zener-like Suppr.	4.9	0	0	0	3	-	100
"	LVC-1Z-1/10A	"	10	0	0	0	3	-	100
"	LVC-1Z-1/20A	"	20	0	0	0	2	-	-
"	LVC-1Z-1/100A	"	100	0	0	0	3	-	100
"	LVC-1Z-1/200A	"	200	0	0	0	2	-	-
"	LVC-1Z-10/10A	"	10	0	0	0	2	-	-
"	LVC-1Z-10/20A	"	20	0	0	0	2	-	-
"	LVC-1Z-10/100A	"	100	0	0	0	2	-	-
"	LVC-1Z-10/200A	"	200	0	0	0	2	-	-
"	LVC-1Z-50/4.9A	"	4.9	0	0	0	2	-	-
"	LVC-1Z-50/10A	"	10	0	0	0	1	-	-
"	LVC-1Z-50/20A	"	20	0	0	0	1	-	-
"	LVC-1Z-50/100A	"	100	0	0	0	1	-	-
"	LVC-1Z-50/200A	"	200	0	0	0	1	-	-

*See table IV for manufacturers names.

TABLE I. INSERTION LOSS INDUCED IN A 50-Ω SYSTEM BY EACH COMMERCIAL DEVICE TESTED. (LOSSES ARE TABULATED AT 5, 10, 50, AND 100 MHz. ALSO INCLUDED ARE 3-dB POINTS, WHERE THE LOSSES COULD BE DETERMINED.) (Cont'd)

Mfr*	Type	Description	V_B	Insertion loss in decibels at (MHz) 5	10	50	100	3 dB Points (MHz) Low	High
GHZ	GC-4020-15	Microwave switching diode	200	0	0	0	2	-	-
"	GC-4021-15	"	200	0	0	0	2	-	-
"	GC-4050-15	"	500	0	0	0	2	-	-
"	GC-4054-15	"	500	0	0	0	2	-	-
"	GC-4100-15	"	100	0	0	0	2	-	-
ALPHA	DS982B	PIN diode	200	0	0	0	1	-	-
"	DS964B	"	100	0	0	0	1	-	-
M. ASSOC.	MA4B200	[illegible] diode	70	0	0	0	2	-	-
RCA	2N3896	Silicon controlled rectifier	100	3	5	12	12	-	5
"	2N3897	"	200	3	5	12	13	-	5
"	2N3898	"	400	4	6	12	11	-	-
"	2N3529	"	400	0	1	4	9	-	30
"	2N3528	"	200	0	2	4	9	-	30
"	2N3669	"	200	5	7	12	10	-	-
"	2N3872	"	400	2	4	13	14	-	6
"	2N3871	"	200	4	6	15	12	-	-
	2N3670		400	4	5	10	10	-	-

*See table IV for manufacturer's names.

TABLE I. INSERTION LOSS INDUCED IN A 50-Ω SYSTEM BY EACH COMMERCIAL DEVICE TESTED. (LOSSES ARE TABULATED AT 5, 10, 50, AND 100 MHz. ALSO INCLUDED ARE 3-dB POINTS, WHERE THE LOSSES COULD BE DETERMINED.) (Cont'd)

Mfr*	Type	Description	V_B (V)	Insertion loss in decibels at (MHz) 5	10	50	100	3 dB Points (MHz) Low	High
MOTOROLA	IN1326	Avalanche diode	105	0	0	1	10	-	70
"	IN714	"	10	0	2	34	8	-	14
"	IN742	"	150	0	0	0	5	-	85
"	IN1314	"	10	0	0	10	10	-	23.5
"	IN738	"	100	0	0	1	10	-	67.5
"	IN702	"	2.6	2	8	13	7	-	5.5
"	IN1322	"	50	0	0	6	14	-	3.3
"	IN1785	"	39	0	2	12	4	-	12
UNITRODE	UZ8220	"	200	0	0	0	4	-	84
"	UZ8210	"	100	0	0	1	7	-	68
"	UZ8850	"	50	0	0	2	11	-	58
"	UZ8824	"	24	0	0	6	28	-	30
"	UZ8810	"	10	0	2	18	14	-	14
"	UZ8806	"	6.8	1	4	49	13	-	8
INT. RECT.	KY2DPF	Bipolar diode	100	4	6	8	6	-	3
"	KY4DPF	"	200	2	3	4	6	-	10
"	KY9DPF	"	500	0	2	3	4	-	50
"	KY17DPF	"	1000	0	1	2	3	-	100

* See Table IV for manufacturers' names.

TABLE I. INSERTION LOSS INDUCED IN A 50-Ω SYSTEM BY EACH COMMERCIAL DEVICE TESTED. (LOSSES ARE TABULATED AT 5, 10, 50, AND 100 MHz. ALSO INCLUDED ARE 3-dB POINTS, WHERE THE LOSSES COULD BE DETERMINED.)(Cont'd)

Mfr*	Type	Description	V_B (V)	Insertion loss in decibels at (MHz) 5	10	50	100	3 dB Points (MHz) Low	High
ECC	GT-60	Thyristor	60	0	0	0	2	-	-
UNITRODE	GA201A	"	50A	0	1	2	7	-	60
"	GA201B	"	50A	0	1	4	9	-	30
TII	300B	Gas-tube arrester	300-500	0	0	0	0	-	-
"	300C	"	500-900	0	0	0	0	-	-
"	300A	"	150-300	0	0	0	0	-	-
SIEMENS	B2-B470	Spark gap	470	0	0	0	0	-	-
"	B2-H25	"	2500	0	0	0	0	-	-
"	B1-C90	"	90	0	0	0	0	-	-
"	KA6	"	6500-9500	0	0	0	0	-	-
"	B1-A350	"	350	0	0	0	0	-	-
"	B1-A230	"	230	0	0	0	0	-	-
"	B1-F90	"	90	0	0	0	0	-	-
"	S2-B800	"	800	0	0	0	0	-	-
"	B1-C145	"	145	0	0	0	0	-	-
"	B2-H10	"	1000	0	0	0	0	-	-

*See table IV for manufacturers names.

TABLE I. INSERTION LOSS INDUCED IN A 50-Ω SYSTEM BY EACH COMMERCIAL DEVICE TESTED. (LOSSES ARE TABULATED AT 5, 10, 50, AND 100 MHz. ALSO INCLUDED ARE 3-dB POINTS, WHERE THE LOSSES COULD BE DETERMINED.) (Cont'd)

Mfr*	Type	Description	V_B (V)	Insertion loss in decibels at (MHz) 5	10	50	100	3 dB Points (MHz) Low	High
JOSLYN	2001-06	Miniature spark gap	230	0	0	0	0	-	-
"	2001-07	"	350	0	0	0	0	-	-
"	2001-08	"	470	0	0	0	0	-	-
"	2001-09	"	800	0	0	0	0	-	-
"	2001-31	"	230	0	0	0	0	-	-
DALE	LA9A1A/300V	Preionized spark gap	300	0	0	0	0	-	-
"	LA9A1A/400V	"	400	0	0	0	0	-	-
"	LA9A1A/500V	"	500	0	0	0	0	-	-
"	LA9A1A/750V	"	750	0	0	0	0	-	-
"	LA9A1A/1000V	"	1000	0	0	0	0	-	-
EG&G	GP-57-6	"	6000	0	0	0	0	-	-
"	GP-44L	"	12500	0	0	0	0	-	-
"	GP-64-4.9	"	4900	0	0	0	0	-	-
TEXSCAN	6BE41.5/23	Bandpass filter	-	50	46	1	78	29	53
"	6BD41.5/23	"	-	46	37	1	78	24	56
"	6BE64.5/23	"	-	73	67	10	77	52	75

*See table IV for manufacturers names.

TABLE I. INSERTION LOSS INDUCED IN A 50-Ω SYSTEM BY EACH COMMERCIAL DEVICE TESTED. (LOSSES ARE TABULATED AT 5, 10, 50, AND 100 MHz. ALSO INCLUDED ARE 3-dB POINTS, WHERE THE LOSSES COULD BE DETERMINED.) (Cont'd)

Mfr*	Type	Description	V_B (V)	Insertion loss in decibels at (MHz) 5	10	50	100	3 dB Points (MHz) Low	High
TEXSCAN	6BD64.5/23	Bandpass filter	-	78	76	10	77	51	76
"	6BE50/40	"	-	39	33	1	78	29	69
"	6BD50/40	"	-	47	39	1	77	29	69
"	6BC64.5/23	"	-	75	72	8	70	51	76
TMC	FIL-0514	Crystal bandpass filter	-	>50	>50	>50	20	-	-
LUNDY	A60-B/60HZ	EMI filter	125V/60A	6	14	>50	>50	-	4
"	A60-B/400HZ	"	"	3	14	>50	>50	-	5
"	A10-B/60HZ	"	125V/10A	8	20	63	63	-	3
"	A20-B/400HZ	"	"	13	19	65	65	-	2.4
"	A2-B/60HZ	"	125V/2A	7	12	25	19	-	2
"	A2-B/400HZ	"	125V/1.5A	6	11	14	22	-	1.4
"	5005-05K-258	Lossy-line filter	500V/5A	0	2	8	17	-	16
SPEC.CONT.	51-715-001	EMI filter	750V/25A	4	8	32	32	-	4
"	51-702-003	"	500V/25A	8	16	40	36	-	2
"	51-714-004	"	200V/10A	15	29	44	46	-	0.7
"	51-714-007	"	100V/10A	28	34	48	50	-	0.2
"	51-301-030	"	50V/10A	58	68	70	66	-	-

*See table IV for manufacturers names.

TABLE I. INSERTION LOSS INDUCED IN A 50-Ω SYSTEM BY EACH COMMERCIAL DEVICE TESTED. (LOSSES ARE TABULATED AT 5, 10, 50, AND 100 MHz. ALSO INCLUDED ARE 3-dB POINTS, WHERE THE LOSSES COULD BE DETERMINED.) (Cont'd)

Mfr*	Type	Description	V_S (V)	Insertion loss in decibels at (MHz) 5	10	50	100	3 dB Points (MHz) Low	High
RTRON	RNC-111	RFI/EMI filter	400V/5A	63	57	44	38	-	.03
"	RNC-124	"	400V/2A	70	58	50	37	-	.01
USCC	2100-026	"	-	74	50	41	35	-	-
"	2100-026A	"	-	73	52	44	38	-	-

*See table IV for manufacturers names.

TABLE II. APPROXIMATE SAFE AND FAILURE PULSE VOLTAGE LEVELS FOR EACH COMMERCIAL DEVICE TESTED. (APPLIED PULSE WIDTHS WERE 50 AND 500 NSEC. A DASH MEANS THAT THE CORRESPONDING LEVEL WAS NOT DETERMINED.)

Mfr	# Tested	Type	Description	V_R (V)	Safe Voltage at 50 nsec (V)	Failure Voltage at 50 nsec (V)	Safe Voltage at 500 nsec (V)	Failure Voltage at 500 nsec (V)
MCG	2	LVC-1PA-6.8	Preset crowbar, dc	6.8	11000	-	11000	
"	2	LVC-1PA-10	"	10	"	-	"	-
"	2	LVC-1PA-15	"	15	"	-	"	-
"	2	LVC-1PA-20	"	20	"	-	"	-
"	2	LVC-1PA-50	"	50	"	-	"	-
"	2	LVC-1PA-100	"	100	3800	8500	-	-
"	2	LVC-1PA-150	"	150	11000	-	7500	11000
"	2	LVC-1PA-200	"	200	"	-	"	"
TRANS-TECTOR	2	VH11DC1	Hybrid SCR crowbar	11	"	"	-	-
"	2	VH16.5DC1	"	16.5	"	"	-	-
"	2	VH30DC1	"	30	1000	8500	-	-
"	2	VH50DC1	"	50	"	"	-	-
"	2	VH5DC1	"	5	0	1000	-	-
DALE	2	LVP-6/6.2V	Avalance diode	6.2	11000	-	11000	-
"	2	LVP-6/7.5V	"	7.5	"	-	"	-
"	2	LVP-6/9.1V	"	9.1	"	-	"	-
"	3	LVP-6/11V	"	11	1000	3800	"	-
"	2	LVP-6/13V	"	13	11000	-	"	-

*Evidently a spurious result. Two of these devices survived at 500 nsec.

TABLE II. APPROXIMATE SAFE AND FAILURE PULSE VOLTAGE LEVELS FOR EACH COMMERCIAL DEVICE TESTED. (APPLIED PULSE WIDTHS WERE 50 AND 500 NSEC. A DASH MEANS THAT THE CORRESPONDING LEVEL WAS NOT DETERMINED.) (Cont'd)

Mfr	# Tested	Type	Description	V_B (V)	Safe Voltage at 50 nsec (V)	Failure Voltage at 50 nsec (V)	Safe Voltage at 500 nsec (V)	Failure Voltage at 500 nsec (V)
GSI	2	1N5017	Avalanche diode	7.5	11000	-	11000	-
"	2	1N5020	"	10	"	-	"	-
"	2	1N5042	"	50	"	-	"	-
"	2	1N5051	"	100	"	-	3500	7500
"	2	1N5344B	"	8.2	"	-	11000	-
"	2	1N5369B	"	51	"	-	7500	11000
"	2	1N5378B	"	100	1000	3000	-	-
"	2	1N5388B	"	200	"	"	-	-
MOTOROLA	2	1N1518	"	3.9	11000	-	-	3500
"	2	1N5262	"	52	3000	8500	-	-
"	2	1N5281	"	200	1000	3000	-	-
"	3	1N5271	"	100	"	"	-	-
"	2	1N5221	"	2.4	3000	9500	-	-
"	2	1N5240	"	10	"	"	-	-
"	2	1N1523	"	10	11000	-	3500	7500
"	2	1N745	"	200	1000	3000	-	-
"	2	1N1799	"	150	3000	8500	-	-

TABLE II. APPROXIMATE SAFE AND FAILURE PULSE VOLTAGE LEVELS FOR EACH COMMERCIAL DEVICE TESTED. (APPLIED PULSE WIDTHS WERE 50 AND 500 NSEC. A DASH MEANS THAT THE CORRESPONDING LEVEL WAS NOT DETERMINED.) (Cont'd)

Mfr	# Tested	Type	Description	V_B (V)	Safe Voltage at 50 nsec (V)	Failure Voltage at 50 nsec (V)	Safe Voltage at 500 nsec (V)	Failure Voltage at 500 nsec (V)
MOTOROLA	2	IN1802	Avalanche diode	200	11000	-	11000	-
"	2	IN1788	"	51	"	-	3500	7500
"	2	IN1326	"	105	3800	8500	-	-
"	2	IN714	"	10	"	"	-	-
"	2	IN742	"	150	"	"	-	-
"	2	IN1314	"	10	"	"	-	-
"	2	IN738	"	100	1000	"	-	-
"	2	IN702	"	2.6	3800	"	-	-
"	2	IN1322	"	50	"	"	-	-
"	2	IN1785	"	39	11000	-	3500	7500
UNITRODE	2	UZ8220	"	200	1000	3800	-	-
"	2	UZ8210	"	100	"	"	-	-
"	2	UZ8850	"	50	"	"	-	-
"	2	UZ8824	"	24	3800	8500	-	-
"	2	UZ8810	"	10	11000	-	3500	7500
"	2	UZ8806	"	6.8	3800	8500	-	-

*Goes into second breakdown or arcs internally.

TABLE II. APPROXIMATE SAFE AND FAILURE PULSE VOLTAGE LEVELS FOR EACH COMMERCIAL DEVICE TESTED. (APPLIED PULSE WIDTHS WERE 50 AND 500 NSEC. A DASH MEANS THAT THE CORRESPONDING LEVEL WAS NOT DETERMINED.) (Cont'd)

Mfr	# Tested	Type	Description	V_B (V)	Safe Voltage at 50 nsec (V)	Failure Voltage at 50 nsec (V)	Safe Voltage at 500 nsec (V)	Failure Voltage at 500 nsec (V)
INT. RECT.	2	KY2DPF	Bipolar diode	100	3800	8500	-	-
"	2	KY4DPF	"	200	"	"	-	-
"	2	KY9DPF	"	500	"	"	-	-
"	2	KY17DPF	"	1000	"	"	-	-
GHZ	2	GC-4020-15	Microwave switching diode	200	0	1000	-	-
"	2	GC-4021-15	"	200	Undet	3800	-	-
"	2	GC-4050-15	"	500	"	"	-	-
"	2	GC-4054-15	"	500	"	"	-	-
"	2	GC-4100-15	"	100	0	1000	-	-
ALPHA	5	DS982B	PIN Diode	200	1000	3800	-	-
"	4	DS964B	"	100	"	"	-	-
M. ASSOC	4	MA4B-200	Pulse shaping diode	70	"	"	-	-

TABLE II. APPROXIMATE SAFE AND FAILURE PULSE VOLTAGE LEVELS FOR EACH COMMERCIAL DEVICE TESTED. (APPLIED PULSE WIDTHS WERE 50 AND 500 NSEC. A DASH MEANS THAT THE CORRESPONDING LEVEL WAS NOT DETERMINED.) (Cont'd)

Mfr	# Tested	Type	Description	V_B (V)	Safe Voltage at 50 nsec (V)	Failure Voltage at 50 nsec (V)	Safe Voltage at 500 nsec (V)	Failure Voltage at 500 nsec (V)
RCA	2	2N3896	Silicon-controlled rectifier	100	1000	3800	-	-
"	2	2N3897	"	200	3800	8500	-	-
"	2	2N3898	"	400	"	"	-	-
"	2	2N3529	"	400	1000	3800	-	-
"	2	2N3528	"	200	0	1000	-	-
"	2	2N3669		200	1000	3800	-	-
"	2	2N3872	"	400	3800	8500	-	-
"	2	2N3871	"	200	"	"	-	-
"	2	2N3670	"	400	"	"	-	-
"	2	40655	"	500	1000	8500	-	-
"	2	40654	"	250	"	"	-	-
ECC	2	GT-40	Diode ac switch	43	1000	8500	-	-
GE	4	ST-2	"	32	0	3800	-	-
RCA	2	1N5411	"	29	11000	-	11000	-

TABLE II. APPROXIMATE SAFE AND FAILURE PULSE VOLTAGE LEVELS FOR EACH COMMERCIAL DEVICE TESTED. (APPLIED PULSE WIDTHS WERE 50 AND 500 NSEC. A DASH MEANS THAT THE CORRESPONDING LEVEL WAS NOT DETERMINED.) (Cont'd)

Mfr	# Tested	Type	Description	V_R (V)	Safe Voltage at 50 nsec (V)	Failure Voltage at 50 nsec (V)	Safe Voltage at 500 nsec (V)	Failure Voltage at 500 nsec (V)
MCG	1	LVC-1Z-1/4.9A	Biased Zener-like suppressor	4.9	DEST CT	BEST CT	-	-
"	1	LVC-1Z-1/10A	"	10	"	"	-	-
"	1	LVC-1Z-1/20A	"	20	1000	3000	-	-
"	1	LVC-1Z-1/100A	"	100	"	"	-	-
"	1	LVC-1Z-1/200A	"	200	"	"	-	-
"	1	LVC-1Z-10/10A	"	10	"	"	-	-
"	1	LVC-1Z-10/20A	"	20	"	"	-	-
"	1	LVC-1Z-10/100A	"	100	BEST CT	BEST CT	-	-
"	1	LVC-1Z-10/200A	"	200	DEST CT	DEST CT	-	-
"	1	LVC-1Z-50/4.9A	"	4.9	1000	3000	-	-
"	1	LVC-1Z-50/10A	"	10	"	"	-	-
"	1	LVC-1Z-50/20A	"	20	"	"	-	-
"	1	LVC-1Z-50/100A	"	100	"	"	-	-
"	1	LVC-1Z-50/200A	"	200	"	"	-	-
ECC	2	GT-60	Thyristor	60	"	"	-	-
UNITRODE	3	GA201A	"	50A	"	"	-	-
"	3	GA201B	"	50A	"	"	-	-

TABLE II. APPROXIMATE SAFE AND FAILURE PULSE VOLTAGE LEVELS FOR EACH COMMERCIAL DEVICE TESTED. (APPLIED PULSE WIDTHS WERE 50 AND 500 NSEC. A DASH MEANS THAT THE CORRESPONDING LEVEL WAS NOT DETERMINED.) (Cont'd)

Mfr	# Tested	Type	Description	V_B (V)	Safe Voltage at 50 nsec (V)	Failure Voltage at 50 nsec (V)	Safe Voltage at 500 nsec (V)	Failure Voltage at 500 nsec (V)
TII	1	300B	Gas-tube arrester	300-500	"	-	"	-
"	1	300C	"	500-900	"	-	"	-
"	1	300A	"	150-300	"	-	"	-
SIEMENS	2	B2-B470	Spark gap	470	11000	-	11000	-
"	2	B2-H25	"	2500	"	-	"	-
"	2	B1-C90	"	90	"	-	"	-
"	2	KA6	"	6500-9500	"	-	"	-
"	2	B1-A350	"	350	"	-	"	-
"	2	B1-A230	"	230	"	-	"	-
"	2	B1-F90	"	90	"	-	"	-
"	2	B2-B800	"	800	11000	-	11000	-
"	2	B1-C145	"	145	"	-	"	-
"	1	B2-H10	"	1000	"	-	"	-
JOSLYN	2	2001-06	Miniature spark gap	230	11000	-	11000	-
"	2	2001-07	"	350	"	-	"	-
"	2	2001-08	"	470	"	-	"	-
"	2	2001-09	"	800	"	-	"	-
"	1	2001-31	"	230	"	-	"	-

TABLE II. APPROXIMATE SAFE AND FAILURE PULSE VOLTAGE LEVELS FOR EACH COMMERCIAL DEVICE TESTED. (APPLIED PULSE WIDTHS WERE 50 AND 500 NSEC. A DASH MEANS THAT THE CORRESPONDING LEVEL WAS NOT DETERMINED.) (Cont'd)

Mfr	# Tested	Type	Description	V_B (V)	Safe Voltage at 50 nsec (V)	Failure Voltage at 50 nsec (V)	Safe Voltage at 500 nsec (V)	Failure Voltage at 500 nsec (V)
DALE	2	LA9A1A/300V	Preionized spark gap	300	11000	-	11000	-
"	2	LA9A1A/400V	"	400	"	-	"	-
"	2	LA9A1A/500V	"	500	"	-	"	-
"	2	LA9A1A/750V	"	750	"	-	"	-
"	2	LA9A1A/1000V	"	1000	"	-	"	-
EG&G	1	GP-57-6	"	6000	11000	-	11000	-
"	1	GP-44L	"	12500	11000	-	11000	-
"	1	GP-64-4.9	"	4900	"	-	"	-
TEXSCAN	1	6BE41.5/23	Bandpass filter	-	11000	-	11000	-
"	1	6BD41.5/23	"	-	"	-	"	-
"	1	6BE64.5/23	"	-	"	-	"	-
"	1	6BD64.5/23	"	-	"	-	"	-
"	1	6BE50/40	"	-	"	-	"	-
"	1	6BD50/40	"	-	"	-	"	-
"	1	6BC64.5/23	"	-	"	-	"	-
TMC	2	FIL-0514	Crystal bandpass filter	-	0	1000	-	-

TABLE II. APPROXIMATE SAFE AND FAILURE PULSE VOLTAGE LEVELS FOR EACH COMMERCIAL DEVICE TESTED. (APPLIED PULSE WIDTHS WERE 50 AND 500 NSEC. A DASH MEANS THAT THE CORRESPONDING LEVEL WAS NOT DETERMINED.) (Cont'd)

Mfr	# Tested	Type	Description	V_R (V)	Safe Voltage at 50 nsec (V)	Failure Voltage at 50 nsec (V)	Safe Voltage at 500 nsec (V)	Failure Voltage at 500 nsec (V)
LUNDY	1	A60-B/60HZ	EMI filter	125V/60A	0	1000	-	-
"	1	A60-B/400HZ	"	"	"	"	-	-
"	1	A10-2/60HZ	"	125V/10A	"	"	-	-
"	1	A20-B/400HZ	"	"	"	"	-	-
"	1	A2-B/60HZ	"	125V/2A	"	"	-	-
"	1	A2-B/400HZ	"	125V/1.5A	"	"	-	-
"	1	5005-05K-155	Lossy-line filter	500V/5A	11000	-	-	-
SPEC.CONT.	2	51-715-001	EMI filter	750V/25A	"	-	7500	11000
"	2	51-702-003	"	500V/25A	"	-	"	(+)
"	2	51-714-004	"	200V/10A	"	-	"	(+)
"	2	51-714-007	"	100V/10A	"	-	"	(+)
"	2	51-301-030	"	50V/10A	"	-	11000	-
RTRON	1	RMC-111	RFI/EMI filter	400V/5A	0	1000	-	-
"	1	RMC-124	"	400V/2A	"	"	-	-
USCC	1	2100-026	"	-	1600	3800	-	-
"	1	2100-026R	"	-	"	"	-	-

* Connector arcs at this level.
(+) Not pulsed at 11 kV because of arcing around device at this level.

The damage data are summarized in table II. Each device is labelled with the highest value of input voltage for which *no* device in that sample sustained damage--this is called the *Safe Voltage*; the lowest value of input voltage for which *any* device in that sample sustained damage is called the *Failure Voltage*. It should be clear that these numbers represent no assurance of performance.

In rare cases the existing data did not permit such an evaluation for a particular device. Some of these cases are labelled with "UNDET" in the appropriate column. In a few other cases the devices were destroyed during curve tracer tests. These are indicated by "DEST CT" in the appropriate column, even though other devices in that sample may have escaped damage until pulsed. For damage evaluation, all such devices were simply considered as untested.

The devices that survived the 11-kV, 50-nsec pulse test include all spark gaps tested, some avalanche diodes, some crowbars, and some filters. Table II shows that the majority of the survivors of the 11-kV, 50-nsec pulse test also survived the 11-kV, 500-nsec pulse test.

4.1.3 Response Time and Overshoot

When a large, fast rise-time pulse was applied to a device, the transmitted voltage momentarily exceeded the rated breakdown voltage of the device, often by several kilovolts. This excess voltage, generally referred to as overshoot, depends on the overall response time of the test system. Operationally, the response time must include the effects of lead inductances--as these cannot be completely separated from the device--and of the test apparatus in addition to the inherent response time of the device. In these tests, the devices were mounted in a way that would minimize the effects of leads and test fixture, which is presumably the way they would be mounted in practice. Since these contributions are not easily separated, the overall response time is the relevant parameter.

Response time was defined for these tests as the difference between the time of arrival of an incident pulse and the time at which the overshoot decayed to one-half of its maximum value. This and other relevant parameters are defined in figure 5 and tabulated for the 11-kV input pulse in table III.

All measured values in table III are averages over the sample of that device type. The clamp voltages are given as upper bounds because they were read from the same photographs as the peak voltages and could not be determined with greater accuracy.

TABLE III. VOLTAGE OVERSHOOT PARAMETERS FOR EACH COMMERCIAL DEVICE THAT SURVIVED ALL 50-NSEC PULSE TESTS. (CORRESPONDING ENERGY LEAKAGES INTO A 50-Ω LOAD ARE ALSO SHOWN.)

Mfr	Type	Description	V_B	Peak Voltage (V)	Clamp Voltage (V)	Rise Time (nsec)	Dwell Time (nsec)	Width (nsec)	Energy Leakage (MJ)
MCG	LVC-1PA-6.8	Preset crowbar, dc	6.8	1155	< 50	1.15	1.30	3.30	0.06
"	LVC-1PA-10	"	10	1000	< 50	1.30	1.50	3.90	0.05
"	LVC-1PA-15	"	15	1080	< 50	1.50	1.30	4.00	0.07
"	LVC-1PA-20	"	20	1055	< 50	1.45	1.55	3.80	0.06
"	LVC-1PA-50	"	50	975	<150	1.40	1.35	4.00	0.07
DALE	LVP-6/6.2V	Avalanche diode	6.2	2355	<100	1.30	1.65	4.40	0.32
"	LVP-6/7.5V	"	7.5	2820	<100	1.40	1.50	4.40	0.47
"	LVP-6/9.1V	"	9.1	2050	<100	1.40	1.60	4.15	0.24
"	LVP-6/13V	"	13	2560	<100	1.65	1.20	3.90	0.37
GSI	1N5017	"	7.5	2615	<100	1.65	1.25	4.45	0.43
"	1N5020	"	10	2205	<100	1.50	1.45	4.50	0.30
"	1N5042	"	50	2565	<200	1.55	1.50	4.45	0.43
"	1N5344B	"	8.2	2155	<100	1.50	1.50	4.50	0.29
"	1N5369B	"	51	2155	<200	1.50	1.55	4.50	0.32
MOTOROLA	1N1518	"	3.9	2260	<150	1.55	1.30	4.60	0.35
"	1N1523	"	10	2025	<100	1.65	1.50	4.65	0.28
"	1N1502	"	200	2560	<209	1.75	1.90	5.45	0.51
"	1N1788	"	51	1995	<300	1.40	1.55	5.50	0.38
"	1N1785	"	39	2250	<250	1.50	1.60	4.80	0.38

TABLE III. VOLTAGE OVERSHOOT PARAMETERS FOR EACH COMMERCIAL DEVICE THAT SURVIVED ALL 50-NSEC PULSE TESTS. (CORRESPONDING ENERGY LEAKAGES INTO A 50-Ω LOAD ARE ALSO SHOWN.) (Cont'd)

Mfr	Type	Description	V_B	Peak Voltage (V)	Clamp Voltage (V)	Rise Time (nsec)	Dwell Time (nsec)	Width (nsec)	Energy Leakage (mJ)
UNITRODE	UZ8810	Avalanche diode	10	2805	<300	1.50	1.35	4.50	0.55
RCA	1N5411	Diode ac switch (DIAC)	29	2335	<100	1.15	1.60	4.20	0.30
TII	300B	Gas-tube arrester	300-500	3900	<300	1.5	1.0	4.1	0.87
"	300C	"	500-900	3900	<300	1.5	1.2	4.2	0.91
"	300A	"	150-300	5200	<300	1.5	1.2	4.2	1.55
SIEMENS	B2-B470	Spark gap	470	3565	<200	1.50	1.50	4.70	0.84
"	B2-H25	"	2500	3660	<200	1.50	1.45	5.15	0.96
"	B1-C90	"	90	2875	<100	1.50	1.45	4.55	0.51
"	KA6	"	6500-9500	10350	<1400	2.10	>23	>23	49.7
"	B1-A350	"	350	3140	<200	1.45	1.45	4.60	0.65
"	B1-A230	"	230	3025	<150	1.40	1.50	4.30	0.55
"	B1-F90	"	90	2820	<100	1.45	1.50	4.25	0.46
"	B2-B800	"	800	5895	<400	1.40	1.50	4.60	2.32
"	B1-C145	"	145	3385	<100	1.65	1.40	4.90	0.71
"	B2-H10	"	1000	3485	<200	1.50	1.50	5.40	0.91

TABLE III. VOLTAGE OVERSHOOT PARAMETERS FOR EACH COMMERCIAL DEVICE THAT SURVIVED ALL 50-NSEC PULSE TESTS. (CORRESPONDING ENERGY LEAKAGES INTO A 50-Ω LOAD ARE ALSO SHOWN.) (Cont'd)

Mfr	Type	Description	V_B	Peak Voltage (V)	Clamp Voltage (V)	Rise Time (nsec)	Dwell Time (nsec)	Width (nsec)	Energy Leakage (MJ)
JOSLYN	2001-06	Miniature spark gap	230	3210	<200	1.30	1.10	3.85	0.58
"	2001-07	"	350	3025	<200	1.30	1.20	3.80	0.51
"	2001-08	"	470	3160	<200	1.40	1.20	4.20	0.61
"	2001-09	"	800	3270	<300	1.40	1.10	4.00	0.68
"	2001-31	"	230	4350	<200	1.40	1.20	3.30	0.90
DALE	LA9A1A/300V	Preionized spark gap	300	3590	<250	1.35	1.05	4.00	0.78
"	LA9A1A/400V	"	400	4150	<250	1.45	1.35	4.15	0.84
"	LA9A1A/500V	"	500	3380	<250	1.50	1.35	4.65	0.78
"	LA9A1A/750V	"	750	4305	<450	1.80	1.10	4.15	1.32
"	LA9A1A/1000V	"	1000	4665	<400	1.65	1.25	4.15	1.42
EG&G	GP-57-6	"	6000	10400	<750	3.80	>7.50	>14.5	18.8
"	GP-64-4.9	"	4900	8820	<500	3.80	>3.80	>10.8	11.4

TABLE III. VOLTAGE OVERSHOOT PARAMETERS FOR EACH COMMERCIAL DEVICE THAT SURVIVED ALL 50-NSEC PULSE TESTS. (CORRESPONDING ENERGY LEAKAGES INTO A 50-Ω LOAD ARE ALSO SHOWN.) (Cont'd)

Mfr	Type	Description	V_B	Peak Voltage (V)	Clamp Voltage (V)	Rise Time (nsec)	Dwell Time (nsec)	Width (nsec)	Energy Leakage (MJ)
TEXSCAN	6BE41.5/23	Bandpass filter	-	[1] 200	-				
"	6BD41.5/23	"	-	[1] 230	-				
"	6BE64.5/23	"	-	[2] 100	-				
"	6BD64.5/23	"	-	[1] 115	-				
"	6BE50/40	"	-	[1] 315	-				
"	6BD50/40	"	-	[1] 230	-				
"	6BC64.5/23	"	-	[1] 115	-				
SPEC CONT	51-715-001	EMI filter	750V/25A	6665	-	33.8	12.4	48.4	22.3
"	51-702-003	"	500V/25A	6455	-	43.5	7.50	54.6	20.3
"	51-714-004	"	200V/10A	3430	-	19.4	3.65	25.9	2.83
"	51-714-007	"	100V/10A	1125	-	37.9	13.3	55.6	0.73
"	51-301-030	"	50V/10A	305	-	1.00	0.50	1.80	0.002

[1] Maximum output voltage observed at 1 kV. Arcs internally at higher voltages.
[2] Arced over externally.

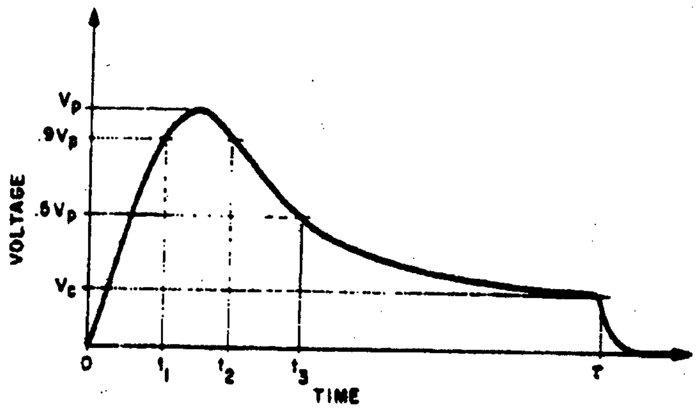

RISE TIME = t_1

DWELL TIME = $t_2 - t_1$

WIDTH = t_3

PULSE DURATION = τ

V_p = PEAK OVERSHOOT VOLTAGE

V_c = CLAMP VOLTAGE OR ARC VOLTAGE

Figure 5. Response time and overshoot parameters for terminal protection devices.

Using measured values of these parameters for the first pulse incident on the device, it is possible to estimate the energy that leaks past the device into a 50-Ω load. The results of such computations are also displayed in table III. Some words of caution are in order with respect to these energy leakages. First, in our test apparatus and to some degree in all real systems, there are reflections at various points, so that more than one pulse will be incident on the device. In our case, the second pulse was larger than the first, often by a factor of 2 or 3. Second, the total heating effect on a semiconductor junction, due to all the leakage pulses, will to some extent be cumulative. This effect will, of course, depend on the separation of the pulses, because of junction cooling between pulses and, thus, on the details of a particular system. At the very least the energy-leakage data of table III provide a convenient basis of comparison for the various devices tested. The method used to calculate these leakage data is given in appendix B. Note that both peak voltage and energy leakage are greater for spark gaps than for most other devices.

4.1.4 Clamp Level

The effectiveness of a protective device is determined in part by its ability to limit the transmitted voltage after the initial overshoot. Thus, the clamp levels of all semiconductor devices that survived all 500-nsec pulse tests were measured under similar conditions. The results are given in table IV. Note that the actual voltage drops are often more than twice the rated breakdown voltage. The energy dissipation in table IV is the product of the maximum current and the breakdown voltage, V_B, which was used for this calculation instead of the clamp voltage. The result is a more conservative estimate of the energy dissipation capacity of that particular device.

4.2 Derivable Quantities

To evaluate the protection offered by a given TPD to a particular circuit with a specified threat level, it is necessary to consider the combination of protector and protected circuit in considerably more detail. This can be done in principle by applying the specified threat to the TPD and using the resulting time-domain waveforms to obtain an equivalent generator for the TPD. This equivalent generator can then be applied to the protected components, and the energy dissipation in each of these components can be evaluated. By this time, there are adequate data from which a prediction of either damage or no damage can be made. A method of obtaining the equivalent circuit of the TPD is given in appendix C. A method for predicting junction damage is given in appendix D and extended to the case of multiple pulses.

4.3 Discussion of Devices

This section summarizes the conclusions obtained from this study relevant to the suitability of various devices as TPD's.

4.3.1 Spark Gaps

Spark gaps still appear to be among the main bulwarks against intrusion of large EMP surges. They are the only protection necessary in some systems. In other systems, they are the only protectors now available with sufficiently small insertion loss.

Spark gaps are available with d-c breakdown voltages varying from about 90 to more than 10,000. The addition of radioactive gases and electrode materials has evidently permitted much faster and more consistent arc formation. These materials can be made with interelectrode capacitances < 1 pF, so that circuit loading is small. Furthermore, they are virtually indestructible by a single EMP transient, with current ratings typically of ~ 10 kA for several microseconds.

TABLE IV. CLAMP VOLTAGE AND APPROXIMATE ENERGY DISSIPATION IN EACH SEMICONDUCTOR DEVICE THAT SURVIVED ALL 500-NSEC PULSE TESTS. (APPLIED PULSE WIDTH WAS ABOUT 580 NSEC.)

Mfr	Type	Description	V_B (V)	Clamp Voltage (V)	Input Voltage (V)	Maximum Current (A)	Energy Diss[1] (mJ)
MCG	LVC-1PA-6.8	Preset crowbar, dc	6.8	16.7	9500	410	4.0
"	LVC-1PA-10	"	10	22.8	"	"	5.4
"	LVC-1PA-15	"	15	26.4	"	"	6.4
"	LVC-1PA-20	"	20	29.9	"	"	7.5
"	LVC-1PA-50	"	50	59.8	"	"	14
DALE	LVP-6/6.2V	Avalanche diode	6.2	10.6	"	"	2.5
"	LVP-6/7.5V	"	7.5	13.2	"	"	3.1
"	LVP-6/9.1V	"	9.1	18.5	"	"	4.4
"	LVP-6/11V	"	11	21.1	"	"	5.0
"	LVP-6/13V	"	13	22.4	"	"	5.3
GSI	IN5017	"	7.5	14.9	"	"	3.5
"	IN5020	"	10	15.8	"	"	3.8
"	IN5042	"	50	101	"	"	24
"	IN5344B	"	8.2	17.6	"	"	4.2

[1]This column gives the total energy dissipated in each device per test pulse.

TABLE IV. CLAMP VOLTAGE AND APPROXIMATE ENERGY DISSIPATION IN EACH SEMICONDUCTOR DEVICE THAT SURVIVED ALL 500-NSEC PULSE TESTS. (APPLIED PULSE WIDTH WAS ABOUT 560 NSEC.) (Cont'd)

Mfr	Type	Description	V_B (V)	Clamp Voltage (V)	Input Voltage (V)	Maximum Current (A)	Energy Diss[1] (mJ)
MOTOROLA	IN1802	Avalanche diode	200	35.2	9500	410	8.4
RCA	IN5411	Diode ac switch	29	31.6	"	"	7.5

[1] This column gives the total energy dissipated in each device <u>per test pulse</u>.
[2] Evidently either second breakdown or internal arcing.

All of the spark gaps tested in this program appear about equally effective for EMP protection. This does not mean that they are equivalent, merely that our test methods could not distinguish between them. The principal drawbacks to using spark gaps are the high d-c breakdown voltage and the relatively high-energy leakage, especially with small overvoltages.

4.3.2 Filters

Two types of filters--bandpass and low pass--were evaluated. In the former category only two different kinds of device were tested. The microwave bandpass filters made by Texscan appeared able to handle the test pulses without damage, and the transmitted voltage waves were small, largely because of arcing somewhere in the device. Such a filter with a relatively narrow passband would probably give adequate protection for some systems.

Of the several low-pass filters tested, only the EMI filters made by Spectrum Control appeared to be undamaged. Generally speaking, these filters passed relatively large amounts of energy. If low leakage is necessary these filters would have to be used in conjunction with or replaced by some other device.

4.3.3 Avalanche Diodes

The avalanche diodes comprise the last major category of devices suitable for terminal protection. Generally speaking, only diodes with low-breakdown voltages can handle the necessary energy, and these diodes have such high-insertion loss as to make them useful only at low frequencies.

There is one scheme for reducing insertion loss of a diode.[*] This method, however, yields a somewhat slower response to a large transient and is ineffective for signal voltages that exceed the forward barrier potential of the compensating diode.

Avalanche diodes can be used extensively to protect low-voltage, low-frequency circuits. Some low-capacitance (microwave) diodes also have potential in combination with other devices that will handle most of the energy, leaving the diode to provide fast clamping of relatively low-level signals in high-frequency circuits.

---

[*] Clark, O. M. and Winters, R. D., General Semiconductor Industries, Inc, "Feasibility Study for EMP Terminal Protection," Final Report, Contract No. DAAG39-72-C-0044.

4.3.4 Miscellaneous Semiconductor Devices

A number of special devices, such as diode a-c switches (DIAC's), crowbars, biased suppressors, silicon-controlled rectifiers (SCR's), thyristors and pin diodes are, in general, of little use for varying reasons. A few of the MCG preset crowbars and the RCA DIAC's survived the pulse tests. Of these, only the DIAC has acceptably low insertion loss above a few hundred kilohertz.

5. CONCLUSIONS

The collection of devices that survived all specified pulse tests principally includes all spark gaps, some bandpass filters, most avalanche diodes with breakdown voltages less than about 50, and a few miscellaneous semiconductor devices with breakdown voltages also less than about 50. The dividing line near 50 V is, no doubt, a function of the maximum current and pulse width used. The devices that survived application of an 11-kV, 500-nsec pulse include almost all survivors of the 50-nsec pulse test.

Of the devices that survived both pulse tests, only spark gaps have acceptably low-insertion loss over the frequency range from 0 to 100 MHz. Therefore, if wide-band protection is needed at the upper end of or beyond the above range, it can at present be provided only by spark gaps.

Spark gaps frequently fire slowly and erratically at overvoltages of less than 2 or 3 times the d-c breakdown voltage. For this reason, they often allow greater energy leakage for small overvoltages than for large overvoltages. Also, because of the arc formation time, spark gaps generally pass somewhat more energy--even when significantly overvolted--than do semiconductor devices, which respond rather rapidly.

The speed of response of each device depends strongly on the method of installation. In fact, examination of table III suggests that the overall response is dominated by such things as lead inductance and the impedance mismatch offered by the test chamber. Other tests have shown that lead inductance is the more important. It is therefore of utmost importance to provide the shortest possible shunt paths for transient currents (except in the case of filters). This implies very small TPD packages with short or no leads.

The bandpass microwave filters manufactured by Texscan offer substantial protection, and these or similar filters may be useful where wide-band response is not necessary.

6. RECOMMENDATIONS

6.1 Individual Devices

When further pulse tests are undertaken, a few carefully selected devices should be examined more closely so that the relevant parameters can be determined with greater precision. The large number of devices used in a survey of this nature does not permit adequate time to test a statistically significant number of each type.

Future experiments should be planned carefully so that the device parameters in the high conduction mode can be derived from the pulse data. These parameters are essential for predicting damage to protected circuits.

A diligent search should be made for a low capacitance device usable at frequencies extending through and somewhat beyond the VHF range. Such a device could supplement or replace the spark gap in many applications.

The usefulness of bandpass filters should be investigated more carefully. This will probably require some sort of survey of the bandwidth requirements of military systems.

6.2 Combinations of Devices

It is likely that no existing single device can provide adequate protection for some systems. The alternative is a combination of devices that complement each other so that the needed protection results. Generally speaking, the combination must have low-insertion loss, be relatively unsusceptible to damage, and provide rapid response to transients, with good voltage clamping ability.

The spark gap appears to be a vital part of any such mixture. It can be put in front of some other device without changing the overall frequency response, while lending its hardness to the whole. The idea is to make the gap fire rapidly, and this usually means a large overvoltage.

Preliminary tests indicate that a spark gap followed by a filter can in some cases provide excellent transient protection for the following reasons:

(a) The frequency content of the input is drastically altered when the spark gap fires. Thus, when the transient is large enough to fire the gap, the energy left in the filter passband may be small, even though the frequency distribution of the original transient was strongly concentrated in the filter passband.

(b) Before the spark gap fires, it can be strongly affected by the portion of the transient that is reflected from the filter. The filter will, in general, reflect a wave composed mainly of frequencies well outside its passband. For such frequencies, the coefficient of reflection for the incident voltage from the filter is essentially +1. The reflected signal will than add constructively to the input signal across the spark gap and speed its turnon. Naturally, the physical separation between spark gap and filter should be small.

The most difficult case for this combination to handle will be when the input transient is concentrated in the filter passband, but the voltage is not large enough to trigger the spark gap during any one-half cycle. This would occur, for example, with a damped sine wave of the form $Ae^{-\delta t}\sin\omega t$, where ω is in the filter passband, δ is not too large, and A is only a few hundred volts. Even in this case, however, the filter output impedance is still roughly that of the input line, which may be large enough to limit the output current to a tolerable value.

It is therefore recommended that the effectiveness of this and other device combinations be determined.

APPENDIX A.--AN ANALYTICAL MODEL FOR THE FAST PULSER USED IN COMPONENT TESTING

Transmission lines may be analyzed by using methods that fall into one of two groups. The methods of the first group use electric circuit theory and have the advantage of analytical simplicity. The parameter values and the conditions under which the resulting equations are applicable, however, must be derived separately.

The methods of the second group depend on electromagnetic theory. They have the advantage of depending directly on the most fundamental principles of macroscopic electrodynamics. These methods also provide all necessary restrictions and approximations and give the parameter values.

Either procedure ultimately results in a pair of coupled first-order equations relating the current and voltage at a particular point on the line. Assuming that the line is balanced--that is, there is no common-mode current, the fundamental transmission-line equations are

$$L \frac{\partial i}{\partial t} + Ri = - \frac{\partial e}{\partial x} ,$$

$$C \frac{\partial e}{\partial t} + Ge = - \frac{\partial i}{\partial x} ,$$

where $i = i(x,t)$ = current in each conductor,

$e = e(x,t)$ = potential difference between conductors,

L = inductance per unit length,

R = resistance per unit length,

C = capacitance per unit length,

G = conductance per unit length.

This appendix follows closely the treatment by Goldman. Laplace transforming the above equations leads to

$$(Ls + R)I(x,s) = - \frac{\partial E(x,s)}{\partial x} + Li(x,0)$$

$$(Cs + G)E(x,s) = - \frac{\partial I(x,s)}{\partial x} + Ce(x,0) .$$

Goldman, Stanford, "Laplace Transform Theory and Electrical Transients," Dover, NJ, 1949.

Preceding page blank

APPENDIX A

These equations are still coupled. Differentiating and substituting give

$$\frac{\partial^2 I}{\partial x^2} - (Ls + R)(Cs + G)\, I = C\,\frac{\partial e(x,o)}{\partial x} - L\,(Cs + G)\, i(x,o)$$

$$\frac{\partial^2 E}{\partial x^2} - (Ls + R)(Cs + G)\, E = L\,\frac{\partial i(x,o)}{\partial x} - C\,(Ls + R)\, e(x,o) \; .$$

Let $n = [(Ls + R)\;(Cs + G)]^{1/2}$. Then the complementary solutions (to the homogeneous equations) are

$$I(x,s) = A_1 e^{-nx} + B_1 e^{nx} \; ,$$

$$E(x,s) = A_2 e^{-nx} + B_2 e^{nx} \; .$$

If we assume no current or voltage on the line at $t = 0$, the complementary functions provide a complete solution.

Now suppose the initial conditions are not quiescent. In particular, consider an initially charged line (fig. A-1), which is a so-called pulse-forming line.

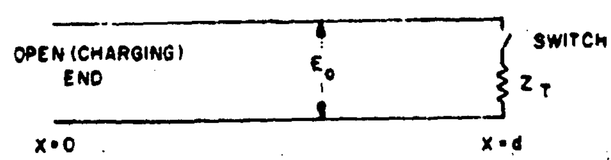

Figure A-1. Circuit diagram of pulse-forming line.

Generally, we have $Z_T = Z_o = \sqrt{L/C}$, a pure resistance called the surge impedance of the line. We assume that $R = G = 0$, which is an excellent approximation in such lines. Then the fundamental equations are

$$\frac{\partial^2 I}{\partial x^2} - s^2 LCI = C\frac{\partial e(x,o)}{\partial x} - LCsi(x,o)$$

$$\frac{\partial^2 E}{\partial x^2} - s^2 LCE = L\frac{\partial i(x,o)}{\partial x} - LCse(x,o) \; .$$

Prior to time t = 0, we have

$$e(x,o) = E_o \ ,$$

$$i(x,o) = 0 \ ,$$

which imply also that

$$\frac{\partial e(x,o)}{\partial x} = \frac{\partial i(x,o)}{\partial x} = 0 \ .$$

Thus, our equations simplify to

$$\frac{\partial^2 I}{\partial x^2} - s^2 LCI = 0 \ ,$$

$$\frac{\partial^2 E}{\partial x^2} - s^2 LCE = -sLCE_o \ .$$

By standard methods of solving differential equations with constant coefficients, we find

$$I(x,s) = A_1 e^{-nx} + B_1 e^{nx}$$

$$E(x,s) = A_2 e^{-nx} + B_2 e^{nx} + \frac{E_o}{s} \ ,$$

where $n = s\sqrt{LC}$. From the form of the fundamental equations in this approximation, we know that

$$I(x,s) = -\frac{1}{sL}\frac{\partial E(x,s)}{\partial x} \ .$$

We therefore find that

$$A_1 = \sqrt{\frac{C}{L}}\, A_2 \ , \quad B_1 = -\sqrt{\frac{C}{L}}\, B_2 \ .$$

From the initial condition at x = 0,

$$I(o,s) = 0 = A_1 + B_1$$

$$\therefore A_1 = -B_1 \ .$$

APPENDIX A

At the other end, for $t > 0$, we have

$$i(d,t) = \frac{e(d,t)}{Z_o} = \sqrt{\frac{C}{L}}\, e(d,t) \quad ,$$

which has the transform

$$I(d,s) = \sqrt{\frac{C}{L}}\, E(d,s) \quad .$$

Our solutions at this end become

$$I(d,s) = A_1\left(e^{-nd} - e^{nd}\right)$$

$$E(d,s) = \sqrt{\frac{L}{C}}\, A_1\left(e^{-nd} + e^{nd} \right) + \frac{E_o}{s} \quad .$$

Using these three relations at $x = d$ we easily find that

$$A_1 = -\frac{1}{2}\sqrt{\frac{C}{L}}\, \frac{E_o}{s}\, e^{-nd} \quad .$$

The solutions in the frequency domain are, therefore,

$$I(x,s) = \frac{1}{2}\sqrt{\frac{C}{L}}\, E_o\left[\frac{e^{-s\sqrt{LC}(d-x)}}{s} - \frac{e^{-s\sqrt{LC}(d+x)}}{s}\right]$$

$$E(x,s) = E_o\left[\frac{1}{s} - \frac{1}{2}\,\frac{e^{-s\sqrt{LC}(d-x)}}{s} - \frac{1}{2}\,\frac{e^{-s\sqrt{LC}(d+x)}}{s}\right] \quad .$$

These are readily transformed back into the time domain. The results are

$$i(x,t) = \frac{1}{2}\sqrt{\frac{C}{L}}\, E_o\left[U\left[t - \sqrt{LC}(d-x)\right] - U\left[t - \sqrt{LC}(d+x)\right]\right]$$

$$e(x,t) = E_o\left\{U(t) - \frac{1}{2}\, U\left[t - \sqrt{LC}(d-x)\right] - \frac{1}{2}\, U\left[t - \sqrt{LC}(d+x)\right]\right\} \quad .$$

where U(t) is a unit step function having the property

$$U(t) = \begin{cases} 0, & t < 0 \\ 1, & t > 0 \end{cases} .$$

The current consists of two step functions that have opposite signs and travel in opposite directions. The first step starts at $x = d$, $t = 0$, and moves to the left. The second step begins at $x = 0$, $t = d\sqrt{LC}$, and moves to the right, cancelling the first as it moves. The net effect is the life history shown in figure A-2.

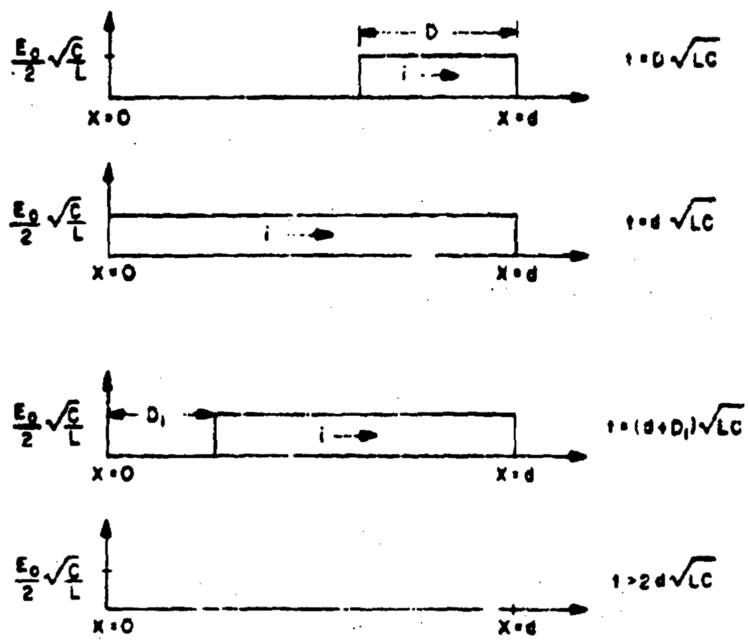

Figure A-2. Life history of current wave in pulse-forming line.

The wavefront travelling to the left can also be considered to be reflected from the open end with a change in sign. All the stored energy is ultimately absorbed in the terminating resistor $R = Z_0$ at $x = d$.

APPENDIX A

The appropriate reflection coefficients are given in a number of standard texts. For voltage,

$$R_v = \frac{Z_T - Z_o}{Z_T + Z_o} ,$$

and for current,

$$R_i = \frac{Z_o - Z_T}{Z_o + Z_T} ,$$

where Z_T is the actual terminating impedance. In the simple cases considered here, we have either $Z_T = Z_o$ or $Z_T = \infty$. The consequent reflection coefficients follow immediately.

Similarly, the voltage consists of three step functions, one stationary in space, one moving to the left, and one to the right. The net effect is the life history shown in figure A-3.

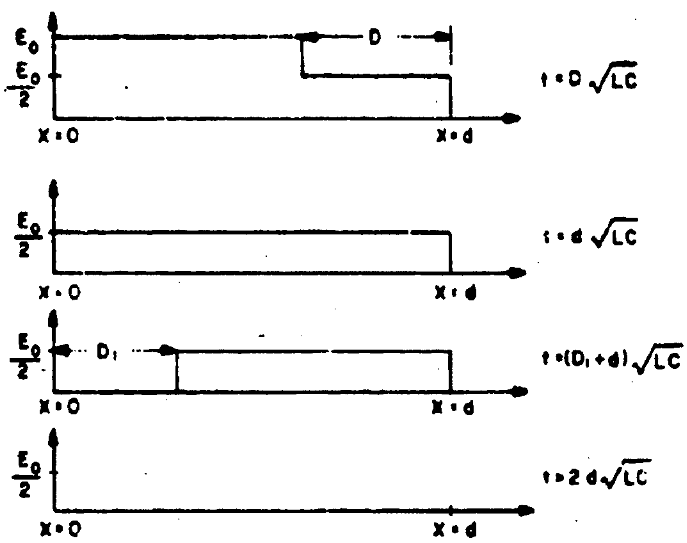

Figure A-3. Life history of voltage wave in pulse-forming line.

APPENDIX A

In this example, the observed voltage at the terminating end is never greater than $E_o/2$.

The energy initially stored in such a line is

$$E = \frac{1}{2}\,(Cd)E_o^2 \quad .$$

On the other hand, if $T = 2d\sqrt{LC}$ is the duration of the pulse, the energy dissipated in R is

$$I^2RT = \left[\frac{1}{2}\sqrt{\frac{C}{L}}\,E_o\right]^2 \sqrt{\frac{L}{C}}\;2d\sqrt{LC} \quad ,$$

$$I^2RT = \frac{1}{2}CdE_o^2 \quad ,$$

which is, of course, in accord with the principle of conservation of energy.

For a coaxial line with air dielectric, the above formulation is valid provided that $a_2 << \lambda$, where a_2 is the i.d. of the outer conductor, and λ is the shortest wavelength of interest.

APPENDIX B.--CALCULATION OF ENERGY LEAKAGE THROUGH TPD INTO A MATCHED LOAD FROM A PULSED INPUT

To compare terminal protection devices in terms of their ability to shield other circuits from large transients, it is useful to calculate the energy leakage into a standard load. For this purpose, the parameters defined in figure 5 (body of report) are reproduced in figure B-1 and connected in a piecewise linear fashion. Familiarity with illustrative pulse data reflects the adequacy of such an approximation.

Referring to figure B-1, the energy deposited in the load R in region 1 is:

$$E_1 = \int_0^{t_1} P_1(t)dt = \frac{V_p^2}{Rt_1^2} \int_0^{t_1} t^2 dt = \frac{V_p^2 t_1}{3R} . \qquad \text{(B-1)}$$

Similarly, for region 2,

$$E_2 = \int_{t_1}^{t_2} P_2(t)dt = \frac{V_p^2}{R} (t_2 - t_1) . \qquad \text{(B-2)}$$

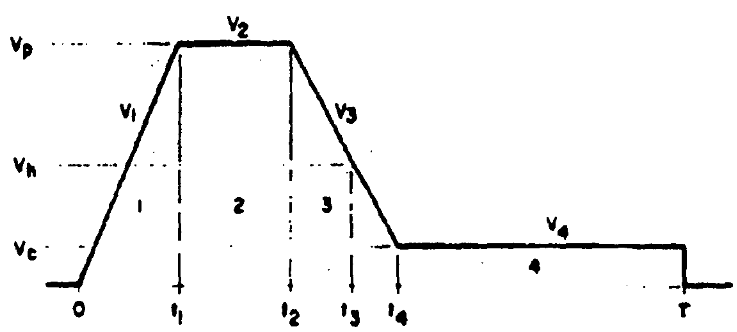

V_h = 0.5 V_p

V_c = CLAMP VOLTAGE

V_p = PEAK OVERSHOOT VOLTAGE

Figure B-1. Approximate output voltage waveform for TPD under pulse test conditions.

Preceding page blank

APPENDIX B

To evaluate E_3, we first need V_3 and t_4 in terms of known quantities. It is easy to discover that

$$V_3(t) = V_p - \frac{V_p}{2}\left(\frac{t - t_2}{t_3 - t_2}\right), \; t_2 \le t \le t_4$$

$$t_4 = t_2 + 2\,(t_3 - t_2)\,\frac{V_p - V_c}{V_p}\,. \qquad \text{(B-3)}$$

The energy E_3 is then

$$E_3 = \int_{t_2}^{t_4} \frac{V_3^2(t)}{R}\,dt = \frac{V_p^2}{R}\int_{t_2}^{t_4}\left[1 - \frac{t-t_2}{2(t_3 - t_2)}\right]^2 dt\,. \qquad \text{(B-4)}$$

A simple change of variable gives

$$E_3 = \frac{V_p^2}{R}\int_0^{t_4-t_2}\left[1 - \frac{u}{2(t_3 - t_2)}\right]^2 du$$

$$E_3 = \frac{2V_p\left(V_p - V_c\right)}{R}\,(t_3 - t_2)\left[1 - \frac{V_p - V_c}{V_p} + \frac{\left(V_p - V_c\right)^2}{3V_p^2}\right]$$

$$E_3 = \frac{2\left(V_p^3 - V_c^3\right)}{3V_p R}\,(t_3 - t_2)\,. \qquad \text{(B-5)}$$

In region 4,

$$E_4 = \int_{t_4}^{\tau} P_4(t)\,dt = \frac{V_c^2}{R}\,(\tau - t_4)$$

$$E_4 = \frac{V_c^2}{R}\left[\tau - t_2 - 2\,(t_3 - t_2)\left(\frac{V_p - V_c}{V_p}\right)\right]\,. \qquad \text{(B-6)}$$

Adding all four components gives the total energy leakage into the load for one pulse.

$$E_T = \frac{V_p^2 t_1}{3R} + \frac{V_p^2}{R}(t_2 - t_1) + \frac{2(V_p^3 - V_c^3)}{3V_p R}(t_3 - t_2)$$

$$+ \frac{V_c^2}{R}\left[\tau - t_2 - \frac{2(V_p - V_c)}{V_p}(t_3 - t_2)\right] . \qquad \text{(B-7)}$$

This can be simplified further for the cases at hand--that is, at the highest input voltages. Here, we always have $V_p > 5V_c$; and in most cases we have $V_p > 10\ V_c$. Hence, we can safely ignore V_c in comparison to V_p. Also, since the V_c^2 term is small, we can approximate it with a more generous estimate by dropping all times except τ.

Then the approximate total energy leakage is

$$E_T = \frac{V_p^2 t_1}{3R} + \frac{V_p^2}{R}(t_2 - t_1) + \frac{2V_p^2}{3R}(t_3 - t_2) + \frac{V_c^2 \tau}{R} . \qquad \text{(B-8)}$$

Since neither t_2 nor $t_3 - t_2$ was directly measured, this can be written in the more convenient form

$$E_T = \frac{V_p^2}{3R}\left[(t_2 - t_1) - t_1 + 2t_3\right] + \frac{V_c^2 \tau}{R} . \qquad \text{(B-9)}$$

The term $t_2 - t_1$ is kept intact because it was directly measured, along with t_1, t_3, and τ.

All times were recorded in nanoseconds; thus, if we want E_T in joules, all terms must be multiplied by 10^{-9}.

APPENDIX C.--ANALYSIS OF EQUIVALENT CIRCUIT OF A DIODE UNDER TEST CONDITIONS

A model for a Zener diode installed in a test system with internal impedance R is shown in figure C-1. Other models have been used for various frequency ranges and conditions of bias. This particular model appears to be the simplest one which is adequate for the large-signal case. The following treatment, adapted from that given by Durgin et al[1] suggests how TPD parameters might be derived when adequate experimental data are available. Other devices might be more or less tractable than the diode.

The diode symbol in figure C-1 represents an ideal diode, that is, it has zero impedance when forward biased, infinite impedance for negative bias between zero and V_Z, and it adjusts its impedance so that the negative bias never exceeds V_Z. The junction capacitance, C, is assumed to be the capacitance at breakdown.

When a positive pulse (negative bias) is applied to this diode, the Zener junction is considered an open circuit until the breakdown voltage, V_Z, is reached with the capacitor, C, charging through L and r. When breakdown occurs the voltage across C ceases to change.

It should be pointed out that the conditions of interest, i.e., fast rise time pulses with V_g one to three orders of magnitude greater than V_Z, are such that the incident voltage exceeds V_Z after a fraction of a nanosecond. Hence, it should be possible to treat this nonlinear device as piecewise linear, that is, to ignore the charging of C and begin measuring time when the diode is far enough into the avalanche region that its resistance is essentially constant and equal to r. In this case the equivalent circuit becomes as shown in figure C-2.

The inductance, L, includes that due to the leads, as well as that inherent in the device. It appears that L, R, and r, together with the rise time of the incident pulse, can adequately account for the observed output voltage. Hence, these parameters should also be sufficient to allow calculation of the source impedance of the terminal protection device, considered as an equivalent generator.

---

[1] Durgin, D. L., [illegible], and [illegible], "Methods, Devices and Circuits for the EMP Hardening of Army Electronics," R&D Tech. Report [illegible], Semiannual Report, Contract No. [illegible].

Preceding page blank

APPENDIX C

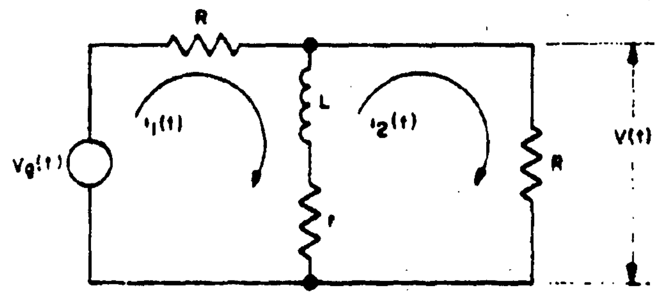

Figure C-1. Equivalent circuit for Zener diode under test conditions.

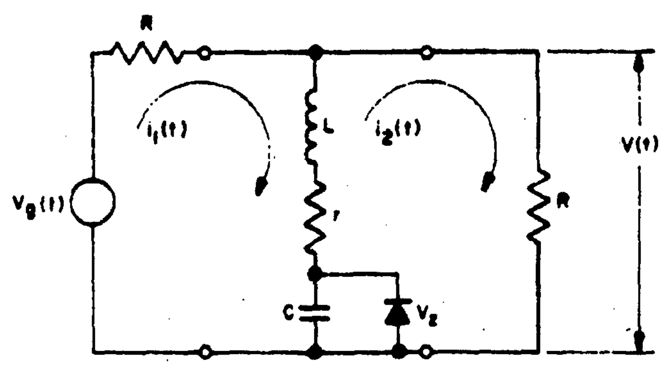

Figure C-2. Reduced equivalent circuit for Zener diode under test conditions.

The loop voltages for the circuit of figure C-2 are:

$$(R + r)i_1 + L\frac{di_1}{dt} \quad ri_2 - L\frac{di_2}{dt} = V_g(t)$$

$$-ri_1 - L\frac{di_1}{dt} + (R+r)i_2 + L\frac{di_2}{dt} = 0 . \qquad \text{(C-1)}$$

The Laplace transforms of these are

$$(R + r + Ls)\, I_1(s) - (r + Ls)\, I_2(s) = V_g(s)$$

$$-(r + Ls)\, I_1(s) + (R + r + Ls)\, I_2(s) = 0 . \qquad \text{(C-2)}$$

Solving for the output current gives

$$I_2 = \frac{V_g(s)\,(r + Ls)}{R(R + 2r + 2Ls)} . \qquad \text{(C-3)}$$

Assuming the input voltage, $V_g(t)$, has an exponential rise with time constant τ,

$$V_g(t) = V_o\left(1 - e^{-t/\tau}\right), \tag{C-4}$$

which transforms to

$$V_g(s) = \frac{V_o}{\tau}\,\frac{1}{s\left(s + \frac{1}{\tau}\right)}\,. \tag{C-5}$$

Setting $R + 2r = 2R'$, I_2 becomes

$$I_2 = \frac{V_o}{2R\tau}\left[\frac{1}{\left(s + \frac{1}{\tau}\right)\left(s + \frac{R'}{L}\right)} + \frac{\frac{r}{L}}{s\left(s + \frac{1}{\tau}\right)\left(s + \frac{R'}{L}\right)}\right]. \tag{C-6}$$

The inverse transform is readily obtained--for example, from the Standard Mathematical Tables, 20th Edition published by the Chemical Rubber Company.

After a little rearranging, we get

$$i_2(t) = \frac{V_o}{2R}\left[\frac{r}{R'} + \frac{L - r\tau}{R'\tau - L}\,e^{-t/\tau} - \frac{[\text{illegible}]\left([\text{illegible}] - \frac{r}{R'}\right)}{R'\tau - L}\,e^{-R't/L}\right]. \tag{C-7}$$

This appears to have the correct form, and it is easy to show that

$$i_2(0) = 0, \quad i_2(\infty) = \frac{V_o r}{R(R + 2r)}\,. \tag{C-8}$$

Furthermore, application of L'Hospital's rule shows that the bracketed sum is bounded when $R'\tau = L$. The output voltage, $V(t)$, is given approximately by

APPENDIX C

$$V(t) = Ri_2(t) + V_z \, .$$

$$V(t) = \frac{V_o}{2}\left[\frac{r}{R'} + \frac{L - r\tau}{R'\tau - L}\, e^{-t/\tau} - \frac{L\left(1 - \frac{r}{R'}\right)}{R'\tau - L}\, e^{-R't/L}\right] + V_z \, .$$

This has the following limits:

$$V(0) = V_z \neq 0, \qquad V(\infty) = \frac{V_o r}{2R'} + V_z \, .$$

The expression for the output voltage can be simplified by considering the approximate values of the parameters.

$R \approx 50\ \Omega \qquad r \approx 1\ \Omega$

$\tau \sim 1\text{-}5$ nsec

$L \sim 10\text{-}50$ nH

$\therefore\ R' = \frac{R + 2r}{2} \approx \frac{R}{2}$

$L - r\tau \approx L$

$$V(t) \approx V_o\left[\frac{r}{R} + \frac{L}{R\tau - 2L}\left(e^{-t/\tau} - e^{-Rt/2L}\right)\right] + V_z \, .$$

In principle, the value of r may be obtained by subtracting V_z from the equilibrium voltage across the diode and dividing the difference by the diode current. Then the values of L and τ may be obtained by fitting the observed waveform to V(t), using the method of least squares. Since R is supposed to be known, L would then be available. The fact that r is actually nonlinear can presumably be fitted into the analysis if desired.

For computing τ and L, neglecting variation in r, it is necessary to observe only the initial overshoot. In this approximation, we have

$$V(t) \approx \frac{V_o L}{R\tau - 2L}\left[e^{-t/\tau} - e^{-Rt/2L}\right] .$$

Since R and V_0 are known, the problem is to find values of C and L so that this expression best fits the observed form.

What is needed, of course, is an equivalent generator for the TPD during application of a large transient. The next step is to apply this generator to the protected circuits to see whether the protection offered by the TPD is adequate. The necessary circuit analysis codes and semiconductor damage data are available elsewhere. Appendix D of parent report gives a method useful where multiple reflections must be considered.

APPENDIX D.--THERMAL RESPONSE OF SEMICONDUCTOR JUNCTIONS UNDER APPLICATION OF A SEQUENCE OF PULSES

D-1. INTRODUCTION

In many electronic systems, an EMP-induced transient effectively consists of a damped sequence of pulses. This condition arises either because of filtering inside the system, or because of multiple reflections from discontinuities in signal transmission paths. The result is that not one pulse but a train of pulses is actually incident on a given TPD. Thus, since the heating effect of the leakage pulses on protected circuits is to some extent cumulative, multiple pulses may raise the temperature of a semiconductor junction to the failure point, even though any one pulse might not be nearly large enough to do so.

A substantial amount of effort, both theoretical and experimental, has been applied to this problem in recent years. The experimental work has consisted mainly of applying a uniform train of rectangular pulses to a device until it fails. The onset of failure is generally announced by second breakdown. The theoretical work has been mostly confined to calculations of temperature rise at certain points in the depletion region. The general procedure is to assume some model for the semiconductor and environs, with heat added homogeneously to the junction during each pulse. The inhomogeneous diffusion equation is then solved for the chosen model, using values of thermal conductivity and diffusivity averaged over the expected temperature range. The predicted junction temperature is compared with the temperature necessary for initiation of second breakdown, which--for unknown reasons--lies very near the intrinsic temperature of the semiconductor.

This appendix presents the results obtained by Minniti[1,2] for a single incident pulse and extended by Frankel[3] to account for an arbitrary number of pulses of known magnitude, width, and separation. The solution is adequate for all pulse widths greater than about 1 nsec and the pulse train can be quite long, possibly as long as 50 μsec, before the heat sink changes temperature appreciably. The responses to sinusoidal and damped sinusoidal inputs are also discussed. Minniti's papers also give a substantial bibliography of the field of thermal breakdown of semiconductor junctions.

---

[1] Minniti, P. J., Jr., "Development of a Semiconductor Failure Model for Lightning Induced Pulses," MDAC-East Avionics Tech. Note ATN 72-001, Dec 1972.

[2] Minniti, R. J., Jr., "Investigation of Second Breakdown in Semiconductor Junction Devices," MDAC-East Avionics Tech. Note ATN 73-002, June 1973.

[3] Frankel, Kenneth A., "A Model for Semiconductor Failure Due to the Application of Multiple Pulses," Fourteenth Annual Student Technical Symposium at HDL, 15-16 Aug 1973.

APPENDIX D

The general line of development in this appendix is to proceed from the simplest model to progressively more realistic models. Some simple, well-known material has been included to make the treatment reasonably self-contained. We are aware that the models employed have defects but hope that the results indicate a viable way of treating the effect of multiple pulses in a given system.

It has been found that junction devices undergo a phenomenon known as "second breakdown" before they fail. In second breakdown, the device operates in a high-current mode with a low-voltage drop across the junction. When a device is in the avalanche mode, it is believed that elevated temperatures will cause current constrictions at defects in the junction. The locally increased current density will further raise the temperature at the weak points. These local hot spots can enlarge the defect, and can cause local melting, which may destroy the device.

Some authors believe that a device will go into second breakdown when any weak spot reaches the intrinsic temperature of the device. At this temperature, the number of thermally-generated instrinsic carriers is equal to the number due to doping of the semiconductor. At the instrinsic temperature, the junction barrier can be destroyed at the weak spot, and most of the current tries to go through this region of low resistance.

Examination of the data for second breakdown caused by single pulses of a given time duration shows that there is a wide range in the power needed to cause second breakdown in devices of a given type. This range often varies by a factor of two or three, and the spread is sometimes an order of magnitude. Such a spread in data is indicative that any general theory developed can at best be an approximation.

Two models used recently by Minniti[1,2] are discussed in the following sections.

D-2. SOLUTION OF DIFFUSION EQUATION FOR N RECTANGULAR INPUT PULSES OF ARBITRARY HEIGHT, WIDTH, AND SEPARATION, USING A SIMPLE ONE-DIMENSIONAL MODEL

Consider the model shown in figure D-1. This simplified model will be used to illustrate the method of solution, the results of which can then be generalized to more complicated cases.

---

[1] Minniti, R. J., Jr., "Development of a Semiconductor Failure Model for Lightning Induced Pulses," MDAC-East Avionics Tech. Note ATN 72-[illegible], Dec 1972.

[2] Minniti, R. J., Jr., "Investigation of Second Breakdown in Semiconductor Junction Devices," MDAC-East Avionics Tech Note ATN 73-002, June 1973.

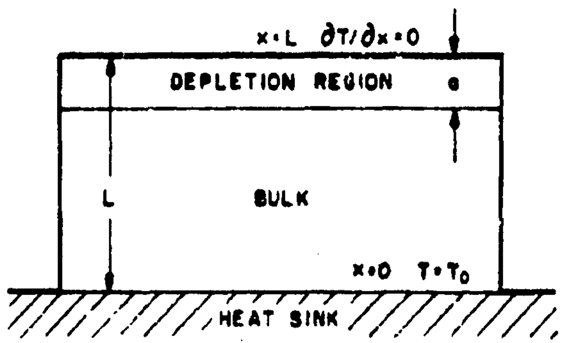

Figure D-1. Simple, one-dimensional thermal model of semiconductor diode.

The initial condition is that the semiconductor and its environment are in thermal equilibrium at temperature T_o.

If the chip temperaure at any point is denoted by $T(x,t)$, the appropriate boundary conditions are

$$T(x,o) = T(o,t) = T_o, \quad \frac{\partial T}{\partial x}\bigg|_{x=L} = 0.$$

The most general form of the diffusion equation is

$$\rho c \frac{\partial T}{\partial t} = \nabla \cdot (K \nabla T) + H(\vec{r}, T, t)$$

where

ρ = density,

c = specific heat,

T = temperature,

t = time,

K = thermal conductivity,

H = heat generated per unit volume per unit time, and

$\vec{r}$ = position vector.

For simplicity, we consider only the case where K is independent of T. This is far from true, of course, but the equation is not otherwise solvable by ordinary analytical means, and numerical solutions are necessary. The diffusion equation can then be written

APPENDIX D

$$\frac{1}{k}\ \frac{\partial T}{\partial t} = \nabla^2 T + \frac{P}{aAK}\ , \qquad \text{(D-1)}$$

where

$k = K/\rho c$ = thermal diffusivity,

P = power input,

a = depletion width, and

A = active area.

Note that the equation now has no dependence on T_o, so the solutions give the temperature rise, $\Delta T = T - T_o$.

To solve the inhomogeneous equation, we first solve the homogeneous equation

$$\frac{1}{k}\ \frac{\partial T}{\partial t} = \frac{\partial^2 T}{\partial x^2}\ , \qquad \text{(D-2)}$$

where we assume that the chip is so large that the y and z dependences of T can be ignored. Using the method of separation of variables we assume a solution of the form

$$\Delta T(x,t) = F(x)G(t),$$

and find

$$F = B\cos\beta x + C\sin\beta x, \qquad G = Ae^{-\beta^2 kt}\ ,$$

where A, B, and C are constants of integration, and $-\beta^2$ is the separation constant.

The boundary condition at $x = 0$ implies that $B = 0$, and the other boundary condition fixes the values of β. We easily find that

$$\beta = (2n-1)\frac{\pi}{2L}\ , \qquad n = \text{positive integer}\ .$$

Thus, the general solution to the homogeneous equation is

$$\Delta T_c(x,t) = \sum_{n=1}^{\infty} D_n e^{-\beta_n^2 kt} \sin\beta_n x\ ,$$

with constants D_n.

The particular integral follows most easily from a modified form of equation (D-1), viz

$$\frac{\partial T}{\partial t} = \frac{K}{\rho c} \nabla^2 T + \frac{H}{\rho c} = k\nabla^2 T + Q \quad . \qquad \text{(D-3)}$$

Now we assume a solution of the form

$$\Delta T = \sum_{n=1}^{\infty} \phi_n(t) \sin n\pi x \quad ,$$

and a heat function of the form

$$Q = \sum_{n=1}^{\infty} Q_n(t) \sin n\pi x \quad . \qquad \text{(D-4)}$$

Putting these into equation (D-3) and using the linear independence of sin [illegible]x, we have for all n

$$\frac{d\phi_n}{dt} + [illegible] k\phi_n = Q_n \quad .$$

This is easily solved using the integrating factor

$$e^{[illegible] kt} \quad ,$$

to multiply both sides; thus, we get

$$\frac{d}{dt}\left[e^{[illegible] kt} \phi_n \right] = Q_n e^{[illegible] kt} \quad .$$

We can next get Q_n by inverting equation (D-4). Since Q is assumed independent of t,

$$Q_n = \frac{2}{L} \int_{L-a}^{L} Q \sin n\pi x dx = \frac{2Q}{[illegible]} \left[-\cos [illegible] x \right]_{L-a}^{L}$$

$$Q_n = \frac{2Q}{L} \sin [illegible] \sin [illegible] \quad ,$$

Putting this into the equation for ϕ_n and noting that $\phi_n(o) = 0$, gives

$$\phi_n(t) = \frac{2Q}{\pi^2 kL}\left(1-e^{-\pi^2 kt}\right)\sin n\pi l \sin n\pi a \ .$$

From equations (D-1) and (D-3), we see that

$$Q = \frac{kP}{aAK} \ ,$$

so the temperature rise is given by

$$\Delta T(x,t) = \frac{2P}{aLAK}\sum_{n=1}^{\infty}\left(1-e^{-\pi^2 kt}\right)$$

$$\frac{1}{\pi^3}\sin n\pi l \ \sin n\pi a \ \sin n\pi x \ . \qquad \text{(D-5)}$$

for a rectangular pulse applied at time 0 and lasting until time t. This result has recently been published by Minniti,[1,2] who also showed that the time dependence reduces to

$$\Delta T \propto t, \quad t < \frac{4a^2}{\pi k}$$

$$\Delta T \propto t^{1/2}, \quad \frac{4a^2}{\pi k} < t < \frac{\pi L^2}{4k}$$

$$\Delta T \propto t^{0}, \quad t > \frac{\pi L^2}{4k} \ .$$

Frankel's contribution[3] was to extend this result to the case of N rectangular pulses of arbitrary height, width, and separation. The solution to the inhomogeneous diffusion equation was given earlier in

---

[1] Minniti, R. J., Jr., "Development of [illegible] Failure Model for Lightning [illegible] Pulses," [illegible] Tech. Note AFWL 72-[illegible], Dec 1972.

[2] Minniti, R. J., Jr., "Investigation of [illegible] Breakdown in [illegible]," [illegible] Tech. Note [illegible] 73-[illegible], [illegible] 1973.

[3] Frankel, [illegible] A., "A [illegible] Failures Due to the Application of Multiple Pulses," [illegible] Annual [illegible] Symposium [illegible], [illegible] 1973.

this section. This solution, equation (D-5), was, of course, only the particular integral, but in that case the complementary function was zero because the initial temperature difference was zero. Thus, the complementary function governs the temperature decay with no excitation present, while the particular integral governs the temperature rise with excitation.

Now suppose that the heat source is turned off at time t_1 the initial condition is given by equation (D-5), with $t = t_1$, and the same boundary conditions exist as before. The solution to the heat equation for this condition was previously given as

$$\Delta T = \sum_{n=1}^{\infty} D_n e^{-\beta^2 kt} \sin\beta x \quad .$$

Since the initial condition is already in Fourier series form, it is evident that the solution at some later time, t_2, is

$$\Delta T(x,t_2) = \frac{2P}{aLAK} \sum_{n=1}^{\infty} \left(1-e^{-\beta^2 kt_1}\right) e^{-\beta^2 k(t_2-t_1)}$$

$$\frac{1}{\beta^2} \sin\beta L \sin\beta a \sin\beta x \quad .$$

Further, suppose that the first pulse was of power P_1 and that at $t = t_2$ a pulse of power P_2 is applied until $t = t_3$. Then we have

$$\Delta T(x,t_3) = \frac{2}{aLAK} \sum_{n=1}^{\infty} \frac{1}{\beta^2} \sin\beta L \sin\beta a \sin\beta x$$

$$\left[P_1\left(1-e^{-\beta^2 kt_1}\right) e^{-\beta^2 k(t_2-t_1)}\right.$$

$$\left. + P_2\left(1-e^{-\beta^2 k(t_3-t_2)}\right)\right] \quad .$$

If there is no pulse until $t = t_2$,

$$\Delta T(x,t_4) = \frac{2}{aLAK} \sum_{n=1}^{\infty} \frac{1}{\lambda_n^2} \sin\lambda_n L \sin\lambda_n a \sin\lambda_n x$$

$$\left[P_1\left(1-e^{-\lambda_n^2 k t_1}\right) e^{-\lambda_n^2 k(t_4-t_2)} + P_2\left(1-e^{-\lambda_n^2 k(t_3-t_2)}\right) e^{-\lambda_n^2 k(t_4-t_3)}\right] .$$

By now it should be easy to see how this goes. After N pulses, we shall have

$$\Delta T\left(x,t_{2N-1}\right) = \frac{2}{aLAK} \sum_{n=1}^{\infty} \frac{1}{\lambda_n^2} \sin\lambda_n L \sin\lambda_n a \sin\lambda_n x$$

$$\sum_{m=1}^{N} P_m \left[1 - e^{-\lambda_n^2 k\left(t_{2m-1}-t_{2m-2}\right)}\right] e^{-\lambda_n^2 k\left(t_{2N-1}-t_{2m-1}\right)} .$$

And after a period of no pulse following N pulses.

$$\Delta T\left(x,t_{2N}\right) = \frac{2}{aLAK} \sum_{n=1}^{\infty} \frac{1}{\lambda_n^2} \sin\lambda_n L \sin\lambda_n a \sin\lambda_n x$$

$$\sum_{m=1}^{N} P_m \left[1 - e^{-\lambda_n^2 k\left(t_{2m-1}-t_{2m-2}\right)}\right] e^{-\lambda_n^2 k\left(t_{2N}-t_{2m-1}\right)} .$$

D-3. SOLUTION FOR N CYCLES OF A SINE-WAVE INPUT, USING A SIMPLE ONE-DIMENSIONAL MODEL

Suppose the input voltage is in the form of a sinusoid. The device voltage is approximately zero when forward biased and approximately V when reverse biased. The current is given by $I = I_o \sin\omega t$ and the power by $P = I_o V \sin\omega t$.

Referring to section D-2, the equation to be solved is

$$\frac{d\theta_n}{dt} + k\lambda_n^2\theta_n = kA_n \sin\omega t ,$$

where

$$A_n = \frac{2I_oV}{aLAK\lambda_n} \sin\lambda_n L \sin\lambda_n a .$$

Using the same integrating factor as before, we find that

$$\phi_n = kA_n \; \frac{\beta^2 k \sin\omega t - \omega\cos\omega t + \omega e^{-\beta^2 kt}}{\beta^4 k^2 + \omega^2} \; .$$

The general solution is then given by

$$\Delta T(x,t) = \frac{2kI_0V}{aLAK} \sum_{n=1}^{\infty} \frac{\sin\beta L \sin\beta a \sin\beta x}{\beta(\beta^4 k^2 + \omega^2)}$$

$$\left[\beta^2 k\sin\omega t - \omega\cos\omega t + \omega e^{-\beta^2 kt}\right]$$

for $t \le \frac{\tau}{2}$, where τ is the period of the sine wave.

After one-half period of such heating,

$$\Delta T(x,\tfrac{\tau}{2}) = \frac{2kI_0V}{aLAK} \sum_{n=1}^{\infty} \sin\beta L \sin\beta a \sin\beta x$$

$$\frac{\omega}{\beta(\beta^4 k^2 + \omega^2)} \left[1 + e^{-\beta^2 k \frac{\tau}{2}}\right] .$$

And after one period, we have

$$\Delta T(x,\tau) = \frac{2I_0Vk}{aLAK} \sum_{n=1}^{\infty} \sin\beta L \sin\beta a \sin\beta x \; ,$$

$$\frac{\omega}{\beta(\beta^4 k^2 + \omega^2)} \left[1 + e^{-\beta^2 k \frac{\tau}{2}}\right] e^{-\beta^2 k \frac{\tau}{2}} \; ,$$

since we assumed that no energy is added when the junction is forward biased.

In general, after N + one-half periods,

$$\Delta T\left(x, \frac{2N+1}{2}\tau\right) = \frac{2I_0Vk}{aLAK} \sum_{n=1}^{\infty} \sin\beta L \sin\beta a \sin\beta x \; .$$

$$\frac{\omega}{\beta(\beta^4 k^2 + \omega^2)} \left[1 + e^{-\beta^2 k \frac{\tau}{2}}\right] .$$

$$\sum_{n=1}^{N} e^{-\beta^2 k n\tau} \; ;$$

whereas after N periods,

$$\Delta T(x, Nt) = \frac{2I_o Vk}{aLAK} \sum_{n=1}^{\infty} \sin n\ldots L \; \sin n\pi a \; \sin n\ldots x$$

$$\frac{[\text{illegible}]}{[\text{illegible}](\ldots + \ldots k\ldots)} \left| 1 + e^{-\ldots k \ldots} \right|$$

$$\sum_{m=1}^{N} e^{-\ldots k(N + \frac{1}{\ldots} - m)\ldots} .$$

D-4. SOLUTION FOR N CYCLES OF A DAMPED SINE-WAVE INPUT, USING A SIMPLE ONE-DIMENSIONAL MODEL

Suppose the input is a damped sine wave. The problem is similar to that of section D-3, except we take

$$I = I_o \, e^{-\ldots t} \sin \ldots t \quad ,$$

so that the equation to be solved is

$$\frac{d\ldots_n}{dt} + \ldots k \ldots_n = kA_n \, e^{-\ldots t} \sin \ldots t,$$

where A_n is the same as in section D-3. The result is

$$\ldots_n = kA_n \, e^{-\ldots kt} \left[\frac{e^{(\ldots k - \ldots)t} \ldots (\beta^2 k - \ldots) \sin \ldots t - \ldots \cos \ldots t \ldots + [\text{illegible}]}{(\ldots k - \ldots)^{\ldots} + \ldots} \right] .$$

This has almost the same form as for the sine wave, the difference being mainly that the $\beta^2 k$ terms of the integrand are replaced by $\ldots k - \ldots$.

After one-half cycle, this becomes

$$\ldots_n = kA_n \ldots \frac{e^{-\ldots \frac{\ldots}{\ldots}} + e^{-\ldots k \frac{\ldots}{\ldots}}}{(\ldots k - \ldots)^{\ldots} + \ldots} .$$

After one cycle,

$$\phi_n = \frac{kA_n}{(\cdot k - \cdot) + \omega}\left(e^{-\cdot\frac{\cdot}{\cdot}} + e^{-\cdot k\frac{1}{2}}\right)e^{-\cdot k\frac{\cdot}{\cdot}} \ .$$

To get the answer for the second period, simply decrease the current by [illegible] and proceed as before. Hence, at $t = \frac{3}{\cdot}$ we get

$$\phi_n = \frac{kA_n}{(\cdot k - \cdot)^{\cdot} + \omega}\left[\left(e^{-\cdot\frac{\cdot}{\cdot}} + e^{-\cdot k\frac{1}{2}}\right)e^{-\cdot k\frac{3}{2}} + \left(e^{-\cdot\frac{\cdot}{\cdot}} + e^{-\cdot k\frac{1}{2}}\right)e^{-\cdot}\right]$$

$$\phi_n = \frac{kA_n}{(\cdot k - \cdot)^{\cdot} + \omega}\left(e^{-\cdot\frac{\cdot}{\cdot}} + e^{-\cdot k\frac{1}{2}}\right)\left(e^{-\cdot} + e^{-\cdot k\frac{3}{2}}\right) \ .$$

In general, after N + one-half periods we can see that

$$\cdot i\left(x, \frac{2N-1}{2}\ \cdot\right) = \frac{2I\ V}{aLAK}\sum_{n=1}^{\cdot} \sin \cdot \sin \cdot \sin \cdot x$$

$$\frac{k\omega}{\cdot(\omega^{\cdot} + (\cdot k - \cdot)^{\cdot})}\left(e^{-\cdot\frac{\cdot}{\cdot}} + e^{-\cdot k\frac{\cdot}{\cdot}}\right) \ .$$

$$\sum_{m=1}^{N} e^{-\cdot k(N-m)\cdot}\ e^{-(m-1)} \ \cdot \ \cdot$$

and after N periods

$$\cdot i(x,N\cdot) = \frac{2I\ V}{aLAK}\sum_{n=1}^{\cdot} \sin \cdot \sin \cdot \sin \cdot x \ \cdot$$

$$\frac{k\omega}{\cdot(\omega^{\cdot} + (\cdot k - \cdot)^{\cdot})}\left(e^{-\cdot\frac{\cdot}{\cdot}} + e^{-\cdot k\frac{\cdot}{\cdot}}\right) \ .$$

$$\sum_{m=1}^{N} e^{-\cdot k(N+1/2-m)\cdot}\ e^{-(m-1)} \ \cdot \ \cdot$$

APPENDIX D

D-5. GENERALIZATION TO MORE COMPLICATED MODELS

The first step in this progressive generalization is shown in figure D-2. Here, a bulk layer is simply added on top of the depletion region. The difference appears in the evaluation of Q_n. In this case we have

$$Q_n = \frac{2}{L}\int_{L-b-a}^{L-b} Q\sin\lambda x\,dx \ .$$

Using a trigonometric identity, we find that

$$Q_n = \frac{2Q}{\lambda L}\,[\cos\lambda L\cos\lambda(a+b) + \sin\lambda L\sin\lambda(a+b)$$

$$- \cos\lambda L\cos\lambda b - \sin\lambda L\sin\lambda b] \ .$$

The boundary condition of $x = L$ requires that $\cos\lambda L=0$. Hence,

$$Q_n = \frac{2Q}{\lambda L}\sin\lambda L\,[\sin\lambda(a+b) - \sin\lambda b] \ .$$

Thus, the only difference between this case and the previous one is the replacement

$$\sin\lambda a \to \sin\lambda(a+b) - \sin\lambda b \ .$$

In subsequent discussions, $\sin\lambda a$ appears whenever complete formulae are required. It will be understood that the extra layer can easily be accounted for if necessary.

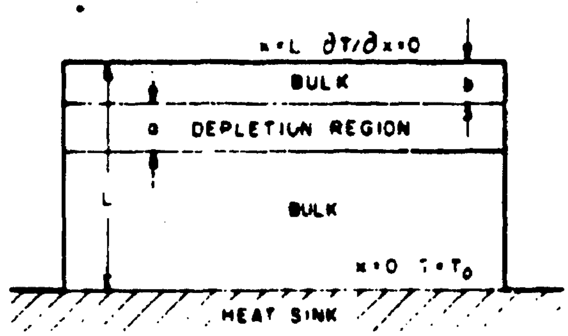

Figure D-2. [illegible]

The final model considered here (fig. D-4) has been treated extensively by Minniti. The solution is derived in essentially the same way as in section D-2, the main complication being that there are now three Fourier expansions instead of one. Thus, we first solve the homogeneous equation

$$\frac{1}{k}\frac{\partial T}{\partial t} = \nabla^2 T = \frac{\partial^2 T}{\partial x^2} + \frac{\partial^2 T}{\partial y^2} + \frac{\partial^2 T}{\partial z^2} \; .$$

by assuming a solution of the form

$$T(\vec{r}, t) = F(x)\, V(y)\, W(z)\, G(t) \; .$$

Proceeding as before we find

$$F = B\cos\alpha x + C\sin\alpha x \; ,$$

$$V = B'\cos\beta y + C'\sin\beta y \; ,$$

$$W = B''\cos\gamma z + C''\sin\gamma z \; .$$

where B, C, B', C', B'', and C'' are constants of integration and $-\alpha^2$, $-\beta^2$, and $-\gamma^2$ are separation constants.

The boundary condition at x = 0 implies that B = 0, and the condition at x = L fixes the value of α as before.

The appropriate boundary conditions on ... [illegible]

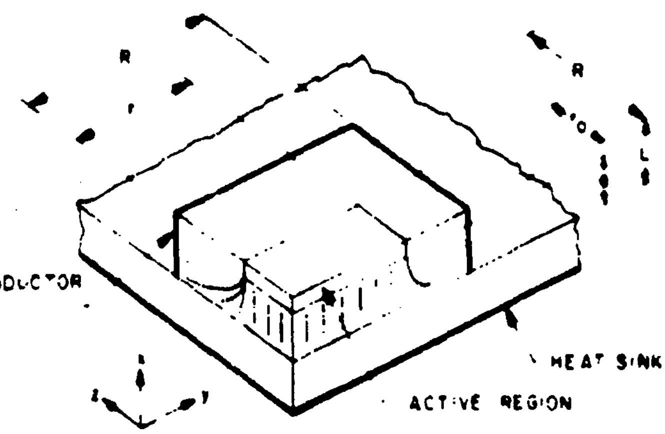

[illegible]

APPENDIX [illegible]

$$\left.\frac{\partial T}{\partial y}\right|_{y=a} = \left.\frac{\partial T}{\partial z}\right|_{z=b} = 0 \; .$$

By symmetry we also see that

$$\left.\frac{\partial T}{\partial y}\right|_{y=0} = \left.\frac{\partial T}{\partial z}\right|_{z=0} = 0 \; .$$

$$\therefore 0 = -B' \sin(aK) + C' \cos aK$$

$$0 = KC' \; .$$

To satisfy both these equations we set $C' = 0$,

$aK = m\pi$, m an integer or zero .

Using the boundary conditions in the z direction, we find $C'' = 0$,

$bK = p\pi$, p an integer or zero .

Finally, the time dependence is given by

[illegible]

Thus, the general solution to the homogeneous equation is

[illegible]

For the particular integral, we assume a solution of the form

[illegible]

where

[illegible]

and a forcing function of the form

[illegible]

Putting these into equation (D-3) as before gives

$$\frac{d\phi_{m,n,p}}{dt} + k(\alpha^2 + \beta^2 + \gamma^2)\phi_{m,n,p} = Q_{m,n,p} \quad .$$

This is solved, using the integrating factor

$$e^{k(\alpha^2+\beta^2+\gamma^2)t}$$

to multiply both sides.

Next, we get $Q_{m,n,p}$ by inverting the equation for Q. We can do this in several steps. For $\beta,\gamma \neq 0$, we get

$$Q_{m,n,p} = \frac{2}{L}\int_{L-a}^{L} \frac{4}{R^2}\int_{0}^{r_i}\int_{0}^{r_i} Q \sin\alpha x \cos\beta y \cos\gamma z \; dx\, dy\, dz$$

$$Q_{m,n,p} = \frac{8Q}{LR^2\alpha\beta\gamma} \sin\alpha L \sin\alpha a \sin\beta r_i \sin\gamma r_i \quad .$$

The y and z integrations [illegible] go to r_i and r_i, because all the energy is assumed to be dissipated in the active region.

For the case $\beta \neq 0$, $\gamma = 0$, we get

$$Q_{m,n,0} = \frac{4Q}{LR^2\alpha} \sin\alpha L \sin\alpha a \int_{0}^{r_i}\int_{0}^{r_i} \cos\beta y \; dy\, dz \;;$$

$$Q_{m,n,0} = \frac{4Qr_i}{LR^2\alpha\beta} \sin\alpha L \sin\alpha a \sin\beta r_i \;;$$

and for the case [illegible], we get

$$Q_{m,0,p} = [illegible] \sin\alpha L \sin\alpha a \sin\gamma r_i \quad .$$

Finally, for [illegible],

$$Q_{m,0,0} = [illegible] \sin\alpha L \sin\alpha a \quad .$$

None of these is dependent on t; thus, our solution becomes

$$\theta_{m,n,p} = \frac{Q_{m,n,p}}{k(\alpha^2+\beta^2+\gamma^2)} \left[1 - e^{-k(\alpha^2+\beta^2+\gamma^2)t} \right] .$$

The general solution for the temperature rise is then

$$\Delta T(\vec{r},t) = \sum_{\substack{m,p=0 \\ n=1}}^{\infty} \frac{Q_{m,n,p}}{k(\alpha^2+\beta^2+\gamma^2)} \left[1 - e^{-k(\alpha^2+\beta^2+\gamma^2)t} \right] .$$

The solutions for all zero and nonzero values of α,β,γ can be combined into one formula if the terms are properly defined. Hence, Minniti gives the general solution

$$\Delta T(\vec{r},t) = \frac{8P}{AKLR^2} \sum_{m,n,p=0}^{\infty} \left[1 - e^{-(\alpha^2+\beta^2+\gamma^2)kt} \right] ,$$

$$\sin\beta L \, \sin\beta a \, \sin\beta x \, \cos\alpha y \, \cos\gamma z ,$$

$$\frac{G(\alpha,\gamma)}{a(\alpha^2+\beta^2+\gamma^2)} ,$$

where $\beta = \frac{2n+1}{2L}$,

$$G(0,0) = \frac{1}{4} r_1 r_2 ,$$

$$G(\alpha,0) = \frac{1}{2\alpha} r_2 \sin\alpha r_1 , \; \alpha \neq 0 ,$$

$$G(0,\gamma) = \frac{1}{2\gamma} r_1 \sin\gamma r_2 , \; \gamma \neq 0 ,$$

$$G(\alpha,\gamma) = \frac{1}{\alpha\gamma} \sin\alpha r_1 \sin\gamma r_2 , \; \alpha,\gamma \neq 0 .$$

This expression is easily extended to give the temperature rise due to N rectangular pulses. At the end of the Nth pulse

APPENDIX D

$$\Delta T\left(\vec{r}, t_{2N-1}\right) = \frac{8}{abLAKR^2} \sum_{m,n,p=0}^{\infty} \sin\alpha L \sin\alpha a \sin\alpha x$$

$$\cos\beta y \cos\gamma z \frac{G(\alpha,\beta,\gamma)}{\alpha(\alpha^2+\beta^2+\gamma^2)} \cdot$$

$$\sum_{i=1}^{N} P_i \left[1 - e^{-(\alpha^2+\beta^2+\gamma^2)k\left(t_{2i-1}-t_{2i-2}\right)} \right]$$

$$e^{-(\alpha^2+\beta^2+\gamma^2)k\left(t_{2N-1}-t_{2i-1}\right)} ;$$

and after a period of no pulse following N pulses,

$$\Delta T\left(\vec{r}, t_{2N}\right) = \frac{8}{abLAKR^2} \sum_{m,n,p=0}^{\infty} \sin\alpha L \sin\alpha a \sin\alpha x$$

$$\cos\beta y \cos\gamma z \frac{G(\alpha,\beta,\gamma)}{\alpha(\alpha^2+\beta^2+\gamma^2)}$$

$$\sum_{i=1}^{N} P_i \left(1 - e^{-(\alpha^2+\beta^2+\gamma^2)k\left(t_{2i-1}-t_{2i-2}\right)}\right)$$

$$e^{-(\alpha^2+\beta^2+\gamma^2)k\left(t_{2N}-t_{2i-1}\right)} .$$

It is easy to show that these expressions reduce to the previous ones when the restrictions on the active area are removed.